Journal Pre-proofs

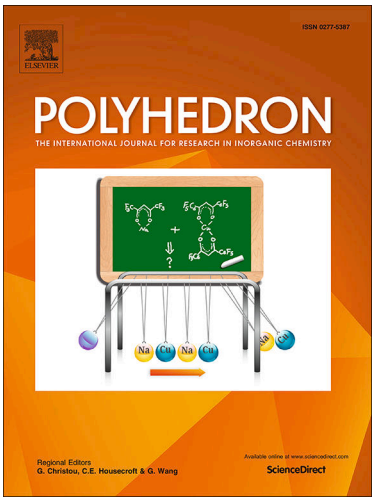

Single monodentate N-donor ligands versus multi-ligand analogues in Pd(II)-catalysed C-C coupling at reduced temperatures

Abiodun Omokehinde Eseola, Helmar Görls, Joseph Anthony Orighomisan Woods, Winfried Plass

PII: S0277-5387(20)30164-9
DOI: https://doi.org/10.1016/j.poly.2020.114507
Reference: POLY 114507

To appear in: *Polyhedron*

Received Date: 6 January 2020
Revised Date: 4 February 2020
Accepted Date: 9 March 2020

Please cite this article as: A.O. Eseola, H. Görls, J.A. Orighomisan Woods, W. Plass, Single monodentate N-donor ligands versus multi-ligand analogues in Pd(II)-catalysed C-C coupling at reduced temperatures, *Polyhedron* (2020), doi: https://doi.org/10.1016/j.poly.2020.114507

Single monodentate N-donor ligands versus multi-ligand analogues in Pd(II)-catalysed C-C coupling at reduced temperatures

Abiodun Omokehinde Eseola,[1,2,*] Helmar Görls,[1] Joseph Anthony Orighomisan Woods,[3] Winfried Plass[1,*]

[1]Institut für Anorganische und Analytische Chemie, Friedrich-Schiller-Universität Jena, Humboldtstr. 8, D-07743 Jena, Germany.
[2]Materials Chemistry group, Department of Chemical Sciences, Redeemer's University Ede, Osun State, Nigeria.
[3]Inorganic Chemistry Unit, Department of Chemistry, University of Ibadan, Ibadan, Nigeria.

Abstract

Deployment of reduced operational temperatures is industrially beneficial and use of the highly efficient, phosphine-based precatalysts is limited by their high costs and inaccessible preparation procedures. In order to study of the influence of coordination environments on catalyst reactivities at reduced temperatures, design of palladium(II) complexes bearing single monodentate N-donor ligands was considered necessary. Consequently, dichloridopalladium(II) complexes of 2-(thiophen-2-yl)-1H-imidazole ligands (**1** – **8**), 2,4,5-triphenyloxazole (**9**) and 2-(1H-imidazol-2-yl)pyridine (**10**) have been prepared, structurally characterized and studied as N-stabilized precatalysts. Ligand donor strengths were spectroscopically estimated by protonation-deprotonation equilibria. The palladium(II) complexes were obtained in three coordination environments; (i) the mono-ligand complexes bearing *trans*-solvent co-ligands (**PdL.acn** and **PdL.dmf**), (ii) the chlorido-bridged dimers **μ-(PdL)$_2$** and (iii) the *trans*-bis-ligand **PdL$_2$** complexes. Considering ambient temperature

* Corresponding authors: Dr. A. O. Eseola:- (a) Institut für Anorganische und Analytische Chemie, Friedrich-Schiller-Universität Jena, Humboldtstr. 8, D-07743 Jena, Germany (b) Materials Chemistry group, Department of Chemical Sciences, Redeemer's University Ede, Osun State, Nigeria; Tel.: +49(0)15218016407, E-mail: biodun.eseola@uni-jena.de; biodun.eseola@tutanota.com
* Prof. Dr. W. Plass; Address:- Institut für Anorganische und Analytische Chemie, Friedrich-Schiller-Universität Jena, Humboldtstr. 8, D-07743 Jena, Germany; Tel.: +49(0)3641 948130; Fax: +49(0)3641948132; e-mail: sekr.plass@uni-jena.de

operations, the catalysis outcomes obtained for the monodentate mono-ligand coordination designs represent an improvement in terms of temperature and reaction time relative to previously reported N-stabilized palladium precatalysts. The mono-ligand pre-catalysts efficiently generate living active palladium species from 40 ^{o}C while a *trans*-bis-ligand phosphine-based pre-catalyst analogue $PdI_2(PPh_3)_2$ displayed no yield under the same temperature conditions. *Trans*-bis-ligand coordination is observed to utterly hinders catalyst efficiencies at the studied temperatures and preformed mono-ligand complexes of mono-dentate N-donors provided positive ligand effects while *in situ* catalyst generation failed. Therefore, the use of multiple ligand equivalents should be discouraged.

Keywords: Catalyst design; Ambient temperatures; N-Donors; Palladium C – C coupling; Ligand effects

Introduction

Palladium-mediated coupling methods have become vital tools in organic syntheses and efforts are still being invested on study of precatalysts systems.[1–3] Current areas of investigation include catalyst development,[4–6] generation of surface-supported catalyst technologies[7–10] and mechanistic studies.[11,12] Numerous sophisticated, ligand-based precatalysts such as PEPPSI^{TM}, AdBrettPhos Pd G3, APhos Pd G2 and XPhos Pd G1 (**Scheme 1 (a)**), which are products of intensive research investigations, have been trademarked.[13–15] However, ligand manipulation is central to catalyst development efforts.[16–18]

While *in situ* approach builds up the catalyst species from 'ligand + palladium salt' ingredients, the preformed palladium complexes often require thermal dissociation of some of the donor arms in order to afford free coordination sites for catalysis (**Scheme 1 (b)**).[19]

Consequently, the energy barrier for decomposition of a precatalyst should depend on donor strengths, chelating character and the manner in which ligands are assembled around the palladium metal centre. Thus, careful selection of coordinating species may aid realization of active precatalyst complexes that do not require high reaction temperatures before freeing up catalytic coordination sites.

These presently high-performing palladium complexes, which are generally phosphine- or organometallic-based,[20–22] have been quite successful in the context of substrate scope and catalytic conversion efficiencies, but the aspect of cost effectiveness could still be improved upon. Several heating hours are also sometimes even necessary for some of them.[23] However, a careful examination of their coordination spheres indicates that only one strong donor function such as phosphine or N-heterocyclic carbene is often bonded on the palladium centre while the remaining donors are generally weaker (**Scheme 1 (a)**). Therefore, it could be imagined that the highly active catalyst forms generated from such precatalyst architectures would consist of mono-ligand monodentate Pd–ligand species. The aim of this paper is to study N-donor palladium(II) precatalyst designs that may generate active species according to the 'one main donor' rational. Furthermore, the common use of multiple ligand-to-palladium equivalents could be seen as ignorant formulations, which are probably responsible for necessity of high temperature for some catalyst systems.[24–26]

The more affordable and stable N-donor ligands have been hitherto less popular as organic backbones for palladium in coupling catalyses. Based on our previous results for azole chelates[27–30] and the few available studies involving monodentate N-donors in palladium-catalysed C-C coupling (**Scheme 1 (c)**),[31–35] this paper aims to investigate possible improvement of catalytic efficiencies for N-stabilized palladium species under ambient temperature regimes.[36–39] Herein, we present results for dichloridopalladium(II) pre-catalysts bearing structurally varied N-donors and coordinated solvents; i.e. 2-(thiophen-2-yl)-

1H-imidazoles **1**–**8**, 2,4,5-triphenyloxazole (**9**) and 2-(1H-imidazol-2-yl)pyridine (**10**) (**Scheme 2**). Comparison with the phosphine complex $PdI_2(PPh_3)_2$ is also reported.

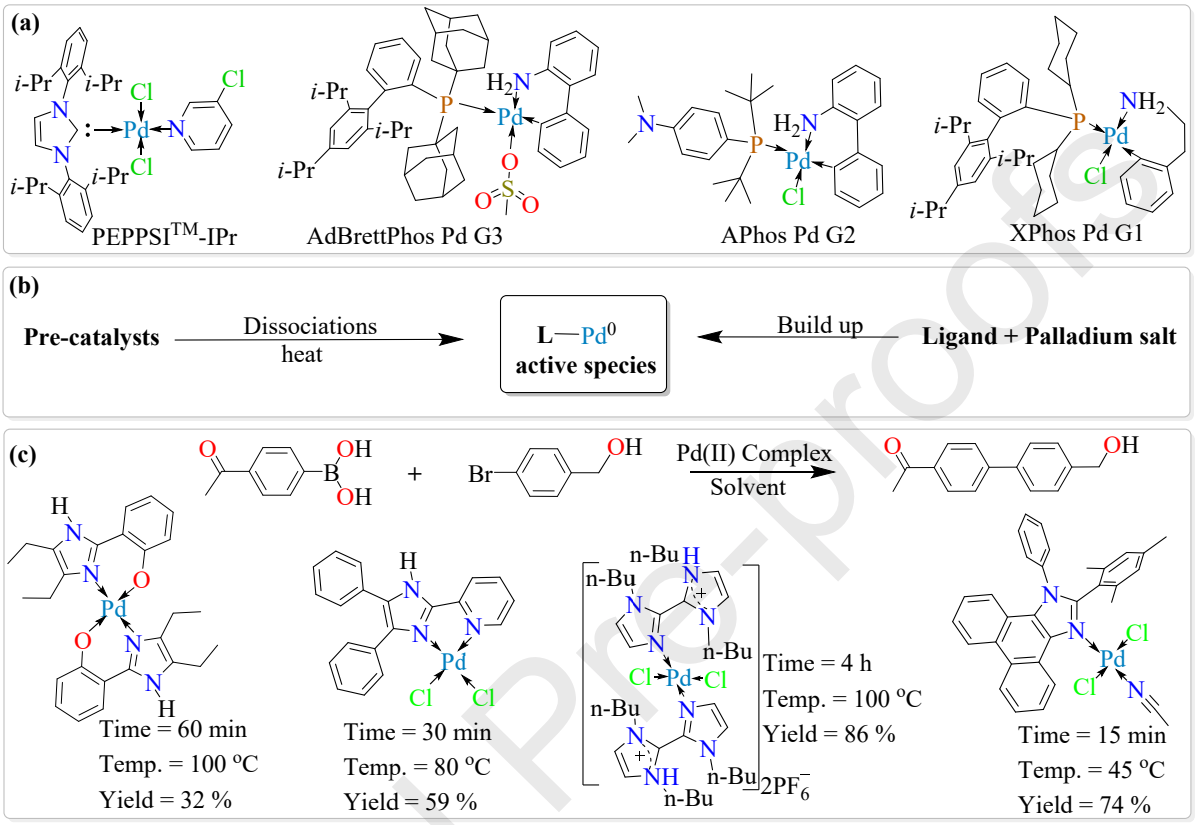

Scheme 1: (a) Some commercialized palladium complex pre-catalysts, **(b)** transformations to active species realization from different catalyst ingredients and **(c)** Some reported catalysis results based on N-donor complexes

Experimental

General information

All starting materials for syntheses as well as substrates for catalytic experiments were obtained commercially as reagent grade and used as supplied. The intermediate pyrene-4,5-dione used for preparation of ligand **1** was prepared according to reported procedure.[40] The ligand 2,4,5-triphenyloxazole (**9**) was obtained as by-product during chromatographic purification of imidazole condensation reactions between benzil and poorly reactive aldehydes.

The complex $PdI_2(PPh_3)_2$ was obtained during column chromatography purification of the product of a Sonogashira reaction in which 10 % catalyst components made up of palladium acetate, CuI and PPh_3 were deployed. In order to exclude impurities in the other synthesized ligands, the organic compounds were routinely purified on silica gel columns. Elemental analyses were performed on Leco CHNS-932 or El Vario III elemental analysers. ^1H and ^{13}C NMR spectra were recorded on Bruker ARX 400 or 600 MHz instrument using deuterated solvents as internal standard. IR spectra were recorded on Shimadzu 8740 FT-IR spectrometer using KBr discs or on Bruker Equinox spectrometer equipped with a diamond ATR unit.

Preparation of the 1H-Imidazolyl ligand analogues

Owing to similarities in the imidazole synthetic procedures, the complete procedure of compound **5** is presented as a typical reaction procedure while the rest report the basic synthetic information details.

1-Phenyl-2-(thiophen-2-yl)-1H-phenanthro[9,10-d]imidazole (5): Thiophene-2-carbaldehyde, (1.08 g, 9.6 mmol), phenanthrene-9,10-dione (2.00 g, 9.6 mmol), aniline (0.89 g, 9.6 mmol) and ammonium acetate (2.20 g, 28.8 mmol) were refluxed for four hours in glacial acetic acid (20 mL). The reaction mixture was cooled, diluted with distilled water and neutralized with aqueous ammonia. The reaction mixture was extracted three times with ethyl acetate and the combined extract purified on silica gel column using 3:10 ethyl acetate / hexane as eluent to obtain ligand **5** as colourless crystals (3.25 g, 89 %). Mp. 233 ^oC. Selected IR peaks (ATR, cm^{-1}): ν 3089m, 3062s, 1610m, 1594s, 1472vs, 1237vs, 697vs, 692vs. ^1H NMR (400 MHz, *d6*-dmso); δ_{ppm} 8.92 (d, J = 8.3 Hz, 1H), 8.87 (d, J = 8.3 Hz, 1H), 8.66 (dd, J = 7.9, 0.9 Hz, 1H), 7.90 – 7.74 (m, 3H), 7.73 – 7.66 (m, 3H), 7.63 (dd, J = 5.0, 0.9 Hz, 1H), 7.60 – 7.51 (m, 2H), 7.34 (t, J = 7.6 Hz, 1H), 7.08 (d, J = 8.1 Hz, 1H), 7.00 (dd, J = 5.0, 3.8 Hz, 1H),

6.71 (dd, *J* = 3.7, 0.9 Hz, 1H). ^{13}C NMR (101 MHz, *d6*-dmso) δ_{ppm} 145.95, 138.25, 136.97, 133.11, 131.47, 131.34, 129.62, 129.05, 128.94, 128.23, 128.21, 128.17, 127.97, 127.27, 127.20, 126.83, 126.33, 125.77, 124.99, 124.16, 122.72, 122.51, 120.45. EI MS: m/z 376 $[M]^+$ (base peak, calc. 376.10).

10-(5-Bromothiophen-2-yl)-9-phenyl-9H-pyreno[4,5-d]imidazole (1): 5-Bromothiophene-2-carbaldehyde (0.82 g, 4.3 mmol), pyrene-4,5-dione (1.00 g, 4.3 mmol), aniline (0.40 g, 4.3 mmol) and ammonium acetate (1.00 g, 12.9 mmol) yielded compound **1**. (1.75 g, 85 %). Mp. 207 ^{o}C. Selected IR peaks (ATR, cm^{-1}): ν 3093m, 3048s, 2956s, 2922vs, 1596vs, 1497vs, 697s. ^{1}H NMR (400 MHz, $CDCl_3$): δ_{ppm} 9.09 (s, 1H), 8.21 – 8.17 (m, 1H), 8.12 (t, *J* = 7.6 Hz, 1H), 8.09 (d, *J* = 8.9 Hz, 1H), 8.02 (t, *J* = 7.7 Hz, 2H), 7.83 (t, *J* = 7.3 Hz, 1H), 7.76 (t, *J* = 7.4 Hz, 2H), 7.69 (d, *J* = 7.2 Hz, 2H), 7.62 (t, *J* = 7.8 Hz, 1H), 7.30 (d, *J* = 7.7 Hz, 1H), 6.89 (d, *J* = 3.9 Hz, 1H), 6.80 (s, br, 1H). ^{13}C NMR (101 MHz, $CDCl_3$): δ 132.17, 131.62, 131.00, 130.80, 130.41, 129.25, 127.98, 127.50, 126.44, 125.40, 124.88, 124.56, 123.52, 122.90, 120.13, 117.66. EI MS: m/z 479 $[M]^+$ (base peak, calc. 478.01).

2-(5-Bromothiophen-2-yl)-1-phenyl-1H-phenanthro[9,10-d]imidazole (2): 5-Bromothiophene-2-carbaldehyde (0.97 g, 4.4 mmol), phenanthrene-9,10-dione (1.00 g, 4.4 mmol), aniline (0.45 g, 4.3 mmol) and ammonium acetate (1.11 g, 14.4 mmol) gave ligand **2** (1.03 g, 51 %). Mp. 179 ^{o}C. Selected IR peaks (ATR, cm^{-1}): ν 3046s, 1612m, 1594s, 1475vs, 1454vs, 752vs, 721vs. ^{1}H NMR (400 MHz, $CDCl_3$); δ_{ppm} 8.89 (d, *J* = 6.5 Hz, 1H), 8.77 (d, *J* = 8.4 Hz, 1H), 8.70 (d, *J* = 8.3 Hz, 1H), 7.83 – 7.72 (m, 3H), 7.68 (t, *J* = 7.7 Hz, 3H), 7.63 (d, *J* = 7.9 Hz, 1H), 7.53 (dd, *J* = 8.2, 7.2 Hz, 1H), 7.27 (dd, *J* = 9.2, 4.8 Hz, 2H), 7.12 (d, *J* = 8.3 Hz, 1H), 6.89 (d, *J* = 3.8 Hz, 1H). ^{13}C NMR (101 MHz, $CDCl_3$): δ_{ppm} 131.00, 129.20, 126.65, 124.22, 123.10, 120.59. EI MS: m/z 454 $[M]^+$ (base peak, calc. 454.01).

2-(5-Bromothiophen-2-yl)-1-(3,4-dimethoxyphenyl)-1H-phenanthro[9,10-d]imidazole (3): 5-Bromothiophene-2-carbaldehyde (0.97, 4.4 mmol), phenanthrene-9,10-dione (1.00 g, 4.4 mmol), 3,4-dimethoxyaniline (0.80 g, 4.4 mmol) and ammonium acetate (1.11 g, 14.4 mmol) yielded compound **3** using 3:10 thf / hexane for silica gel chromatography (1.64 g, 66 %). Mp. 223 ^{o}C. Selected IR peaks (ATR, cm^{-1}): ν 3083m, 3003s, 2944s, 1609m, 1597s, 1511vs, 753vs, 725vs. ^{1}H NMR (400 MHz, $CDCl_3$); δ_{ppm} 8.84 (s, 1H), 8.73 (d, J = 8.3 Hz, 1H), 8.66 (d, J = 8.3 Hz, 1H), 7.72 (t, J = 7.1 Hz, 1H), 7.63 (t, J = 7.6 Hz, 1H), 7.51 (t, J = 7.6 Hz, 1H), 7.29 (t, J = 7.6 Hz, 1H), 7.25 – 7.10 (m, 4H), 7.02 (d, J = 2.2 Hz, 1H), 6.90 (d, J = 3.6 Hz, 1H), 4.08 (s, 3H), 3.86 (s, 3H). ^{13}C NMR (101 MHz, $CDCl_3$): δ_{ppm} 124.15, 123.07, 121.52, 120.62, 111.94, 111.56, 56.38, 56.26. EI MS: m/z 514 $[M]^+$ (base peak, calc. 514.04).

1-(3,4-Dimethoxyphenyl)-2-(thiophen-2-yl)-1H-phenanthro[9,10-d]imidazole (4): Thiophene-2-carbaldehyde (1.08 g, 9.6 mmol), phenanthrene-9,10-dione (2.00 g, 9.6 mmol), 3,4-dimethoxyaniline (1.47 g, 9.6 mmol) and ammonium acetate (2.20 g, 28.8 mmol) produced ligand **4** (1.89 g, 45 %). Mp. 249 ^{o}C. Selected IR peaks (ATR, cm^{-1}): ν 3114m, 3077m, 2998m, 2837m, 1595s, 1512vs, 1021vs, 722vs. ^{1}H NMR (400 MHz, *d6*-dmso); δ_{ppm} 8.91 (d, J = 8.3 Hz, 1H), 8.87 (d, J = 8.3 Hz, 1H), 8.68 – 8.63 (m, 1H), 7.77 (t, J = 7.3 Hz, 1H), 7.71 – 7.66 (m, 1H), 7.63 (dd, J = 5.1, 0.9 Hz, 1H), 7.56 (t, J = 7.2 Hz, 1H), 7.44 – 7.38 (m, 2H), 7.24 (d, J = 8.0 Hz, 1H), 7.05 (dd, J = 5.0, 3.8 Hz, 1H), 6.90 (dd, J = 3.7, 0.9 Hz, 1H), 3.97 (s, 1H), 3.75 (s, 1H). ^{13}C NMR (101 MHz, *d6*-dmso): δ_{ppm} 150.79, 150.56, 146.33, 136.78, 133.18, 130.44, 128.94, 128.85, 128.33, 128.27, 128.17, 127.89, 127.38, 127.32, 126.88, 126.22, 125.70, 124.87, 124.14, 122.90, 122.48, 121.67, 120.65, 112.90, 112.81, 56.53, 56.26. EI MS: m/z 436 $[M]^+$ (base peak, calc. 436.12).

2-(5-Methylthiophen-2-yl)-4,5-diphenyl-1H-imidazole (6): Benzil (1.00g, 4.8 mmol), 5-methythiophene-2-carboxaldehyde (0.72g, 5.7mmol) and ammonium acetate (5.50g, 71.6mmol) formed ligand **6** after dichloromethane extraction and column chromatography by ethyl acetate / hexane (1:2) (0.88 g, 59 %). Mp. 226 ^{o}C. Selected IR peaks (ATR, cm^{-1}): ν 3057s, 1664vs, 1592vs, 1449vs, 765s. ^{1}H NMR (400 MHz, *d6*-dmso): δ_{ppm} 12.66 (s, 1H), 7.50 – 7.39 (m, 7H), 7.38 – 7.31 (m, 1H), 7.28 (t, *J* = 7.4 Hz, 2H), 7.20 (t, *J* = 7.3 Hz, 1H), 6.81 (dd, *J* = 3.5, 1.1 Hz, 1H), 2.46 (s, 3H). ^{13}C NMR (101 MHz, *d6*-dmso): δ_{ppm} 141.74, 139.77, 136.66, 134.91, 131.56, 130.94, 128.74, 128.50, 128.35, 128.28, 128.24, 127.81, 127.51, 127.09, 126.61, 126.25, 124.27, 15.01. EI MS: m/z 316 $[M]^{+}$ (base peak, calc. 316.10).

2-(5-Bromothiophen-2-yl)-4,5-diphenyl-1H-imidazole (7): Benzil (1.00 g, 4.8 mmol), 5-bromo-2-thiophenecarboxaldehyde (0.91 g, 4.8 mmol) and ammonium acetate (7.33 g, 95.1 mmol) in acetic acid (10 mL) afforded ligand **5** after silica gel chromatography by 1:4 ethyl acetate / hexane (1.09 g, 60 %). Mp 228 ^{o}C. Selected IR peaks (ATR, cm^{-1}): ν 3049m, 2960s, 2923vs, 2742s, 1653s, 1591s, 1494vs, 696vs. ^{1}H NMR (400 MHz, *d6*-dmso): δ_{ppm} 12.88 (s, 1H), 7.53 – 7.42 (m, 7H), 7.40 (d, *J* = 6.7 Hz, 1H), 7.30 (dd, *J* = 15.7, 5.6 Hz, 3H), 7.24 (d, *J* = 7.1 Hz, 1H). ^{13}C NMR (101 MHz, d6-dmso): δ_{ppm} 140.97, 137.45, 136.18, 135.02, 131.81, 131.13, 129.23, 128.76, 128.72, 128.47, 127.53, 127.21, 125.00, 111.97. EI MS: m/z 380 $[M]^{+}$ (base peak, calc. 380.00).

4,5-Bis(4-methoxyphenyl)-2-(thiophen-2-yl)-1H-imidazole (8): 1,2-bis(4-methoxyphenyl)ethane-1,2-dione (0.87 g, 3.2 mmol), thiophene-2-carbaldehyde (0.36 g, 3.2 mmol), methyl 4-aminobenzoate (0.37 g, 3.2 mmol) and ammonium acetate (0.74 g, 9.6 mmol) formed compound **8**, but chromatography purification on silica gel was deployed using 1:4 of ethyl acetate / hexane (0.21 g, 18 %). Mp. 177 ^{o}C. Selected IR peaks (ATR, cm^{-1}): ν 2960s,

2835m, 1614s, 1574m, 1501vs, 1246vs, 832vs, 701s. ^{1}H NMR (400 MHz, d6-dmso); δ_{ppm} 12.61 (s, 1H), 7.65 (dd, *J* = 3.6, 0.9 Hz, 1H), 7.53 (dd, *J* = 5.0, 0.8 Hz, 1H), 7.42 (d, *J* = 8.4 Hz, 4H), 7.14 (dd, *J* = 5.0, 3.7 Hz, 1H), 6.94 (d, *J* = 17.8 Hz, 2H), 3.78 (s, 6H). ^{13}C NMR (101 MHz, *d6*-dmso): δ 141.4, 134.7, 128.3, 126.4, 124.3, 114.4, 55.6. EI MS: m/z 362 $[M]^+$ (base peak, calc. 362.11).

2-Bromo-6-(4,5-diphenyl-1H-imidazol-2-yl)pyridine (10): Benzil (1.00 g, 4.8 mmol), 6-bromopicolinaldehyde (0.88 g, 4.8 mmol) and ammonium acetate (7.34 g, 95.2 mmol) gave ligand 10 after dichloromethane extraction and purification by 1:6 ethyl acetate / hexane (0.40 g, 22 %). Mp. 245 ^{o}C. Selected IR peaks (ATR, cm^{-1}): ν 3059m, 1578s, 1554s, 1445vs, 765vs, 606vs. ^{1}H NMR (400 MHz, d6-dmso); δ_{ppm} 13.18 (s, 1H), 8.12 (d, *J* = 7.7 Hz, 1H), 7.84 (t, *J* = 7.8 Hz, 1H), 7.61 (d, *J* = 7.8 Hz, 1H), 7.50 (t, *J* = 7.3 Hz, 4H), 7.43 – 7.36 (m, 3H), 7.30 (t, *J* = 7.4 Hz, 2H), 7.23 (t, *J* = 7.1 Hz, 1H). ^{13}C NMR (101 MHz, *d6*-dmso): δ_{ppm} 149.75, 143.83, 140.95, 140.34, 138.22, 128.91, 128.42, 128.23, 128.02, 127.19, 126.78, 119.26. EI MS: m/z 375 $[M]^+$ (base peak, calc. 375.04).

Synthesis of palladium pre-catalysts

The palladium complexes were obtained either by (i) stirring a mixture of a given ligand and $PdCl_2(CH_3CN)_2$ at room temperature in ethanol (or 1:1 ethanol/chloroform to aid solubility of **5** for ***μ*-(Pd5)$_2$**) or by (ii) isolation of self-assembled crystals from vials where a given ligand and $PdCl_2(CH_3CN)_2$ were layered with a given solvent. Since similar preparative procedures were utilized, the procedure for preparation of complex ***μ*-(Pd1)$_2$** is reported as typical, while the analytical data for each complex species obtained are listed below:

***μ*-(Pd1)$_2$:** Ligand **1** (76 mg, 0.16 mmol), $PdCl_2(CH_3CN)_2$ (40 mg, 0.16 mmol) were placed into a round bottomed flask. Ethanol (1 mL) was added and the reaction mixture was stirred for 2 hours at room temperature. The precipitated complex was filtered under suction and washed with ethanol. The filtered complex was then air dried to obtain ***μ*-(Pd1)$_2$** (80 mg, 80 %). Mp. (with decomposition) 353 ^oC. Selected IR peaks (ATR, cm^{-1}): ν 3203s, 1594s, 1498vs, 970s, 680vs, 450vs. ^1H NMR (400 MHz, *d6*-dmso): δ 8.90 – 8.84 (m, 1H), 8.30 (d, *J* = 6.9 Hz, 1H), 8.18 (m, 4H), 7.87 (m, 5H), 7.73 (t, *J* = 7.9 Hz, 1H), 7.27 (d, *J* = 8.0 Hz, 1H), 7.16 (d, *J* = 4.0 Hz, 1H), 6.56 (d, *J* = 4.0 Hz, 1H). ESI MS: m/z 1,279 $[M - Cl]^+$ (15 %, calc. 1,277.98), 479 (base peak, ligand). Anal. calc. for $C_{54}H_{30}Br_2Cl_4N_4Pd_2S_2$: C, 49.38; H, 2.30; N, 4.27; S, 4.88 %. Found: C, 49.26; H, 2.29; N, 4.12; S, 4.72 %. Crystals of **Pd1.acn** self-assembled in acetonitrile. Mp. (with decomposition) 346 ^oC. Selected IR peaks (ATR, cm^{-1}): ν 3062m, 2918m, 2332m (CH_3CN), 2249m (CH_3CN), 1594s, 1496vs, 705vs, 451vs. Anal. calc. for $C_{31}H_{21}BrC_{l2}N_4PdS$: C, 50.40; H, 2.86; N, 7.58; S, 4.34 %. Found: C, 50.76; H, 2.85; N, 7.49; S, 4.24 %.

***μ*-(Pd2)$_2$:** Ligand **2** (80 mg, 0.18 mmol), $PdCl_2(CH_3CN)_2$ (46 mg, 0.18 mmol) gave ***μ*-(Pd2)$_2$** (100 mg, 91 %). Mp. (with decomposition) 356 ^oC. Selected IR peaks (ATR, cm^{-1}): ν 3062m, 1594s, 1496vs, 765vs, 712vs. ^1H NMR (400 MHz, *d6*-dmso) δ 8.90 (d, *J* = 8.4 Hz, 1H), 8.85 (d, *J* = 8.3 Hz, 1H), 8.61 (dd, *J* = 7.9, 1.2 Hz, 1H), 7.88 – 7.74 (m, 6H), 7.71 – 7.64 (m, 1H), 7.54 (dd, *J* = 11.3, 4.1 Hz, 1H), 7.32 (t, *J* = 7.7 Hz, 1H), 7.12 (d, *J* = 4.0 Hz, 1H), 7.05 (d, *J* = 7.6 Hz, 1H), 6.48 (d, *J* = 4.0 Hz, 1H). ESI MS: m/z 1,230 $[M - Cl]^+$ (10 %, calc. 1,228.94), 457 (base peak, ligand). Anal. calc. for $C_{50}H_{30}Br_2Cl_4N_4Pd_2S_2$: C, 47.46; H, 2.39; N, 4.43; S, 5.07 %. Found: C, 47.07; H, 2.33; N, 4.41; S, 5.06 %. **Pd2.acn** crystals self-assembled in acetonitrile. Mp. (with decomposition) 283 ^oC. Selected IR peaks (ATR, cm^{-1}): ν 3060m, 2916m, 2340m (CH_3CN), 2313m (CH_3CN), 1594s, 1495vs, 700vs. Anal. calc. for

$C_{27}H_{18}BrCl_2N_3PdS$: C, 48.13; H, 2.69; N, 6.24; S, 4.76 %. Found: C, 48.40; H, 2.69; N, 6.14; S, 4.80 %. **Pd2.dmf** was also isolated by allowing **2** and $PdCl_2(CH_3CN)_2$ to stand in dimethylformamide (dmf). Mp. 112 °C. Selected IR peaks (ATR, cm^{-1}): ν 3062m, 2962m, 1655vs (carbonyl of dmf), 1594m, 1389s, 1093s, 766vs, 707vs. Anal. calc. for $C_{28}H_{22}BrCl_2N_3OPdS.2dmf.H_2O$: C, 46.94; H, 4.40; N, 8.15; S, 3.69 %. Found: C, 46.39; H, 4.47; N, 8.58; S, 3.29 %.

$Pd3_2$: Ligand **3** (115 mg, 0.22 mmol) and $PdCl_2(CH_3CN)_2$ (15 mg, 0.11 mmol) produced **$Pd3_2$** (83 %). Mp. 360 °C. Selected IR peaks (ATR, cm^{-1}): ν 3062m, 2932m, 2331w (CH_3CN), 2248w (CH_3CN), 1659vs, 705s. NMR (600 MHz, *d6*-dmso) δ 8.90 (d, *J* = 8.3 Hz, 1H), 8.86 (d, *J* = 8.4 Hz, 1H), 8.62 (dd, *J* = 7.9, 1.1 Hz, 1H), 7.76 (dd, *J* = 11.0, 4.0 Hz, 1H), 7.71 – 7.66 (m, 1H), 7.59 – 7.53 (m, 1H), 7.45 – 7.38 (m, 1H), 7.32 (d, *J* = 1.1 Hz, 2H), 7.20 (d, *J* = 7.5 Hz, 1H), 7.17 (d, *J* = 4.0 Hz, 1H), 6.65 (d, *J* = 4.0 Hz, 1H), 3.96 (s, 3H), 3.74 (s, 3H). ESI MS: m/z 1172 $[M - Cl]^+$ (35 %, Calc. 1,1172.72), 516 (base peak, ligand). Anal. calc. for $C_{54}H_{38}Br_2Cl_2N_4O_4PdS_2.½CH_3CN$: C, 53.76; H, 3.24; N, 5.13; S, 5.22 %. Found: C, 53.99; H, 2.85; N, 5.19; S, 5.74 %.

***μ*-$(Pd4)_2$:** Ligand **4** (71 mg, 0.2 mmol) and $PdCl_2(CH_3CN)_2$ (40 mg, 0.2 mmol) were stirred in ethanol to produced ***μ*-$(Pd4)_2$** (90 mg, 90 %). Mp. 312 °C. Selected IR peaks (ATR, cm^{-1}): ν 3071m, 2928m, 1658vs, 1514s, 1247vs, 756vs, 708vs. NMR (400 MHz, *d6*-dmso) δ 8.87 (dd, *J* = 18.9, 8.3 Hz, 2H), 8.63 (d, *J* = 7.9 Hz, 1H), 7.76 (t, *J* = 7.4 Hz, 1H), 7.70 – 7.64 (m, 1H), 7.61 (dd, *J* = 5.1, 1.0 Hz, 1H), 7.55 (t, *J* = 7.6 Hz, 1H), 7.40 (dd, *J* = 4.5, 2.7 Hz, 2H), 7.29 (d, *J* = 3.2 Hz, 2H), 7.21 (d, *J* = 8.3 Hz, 1H), 7.03 (dd, *J* = 5.0, 3.8 Hz, 1H), 6.89 (dd, *J* = 3.7, 0.9 Hz, 1H), 3.95 (s, 3H), 3.73 (s, 3H). ESI MS: m/z 979 $[M - 2Cl]^+$ (45 %, calc. 978.15), 436 (100 %, ligand). Anal. calc. for $C_{54}H_{40}Cl_4N_4O_4Pd_2S$: C, 52.83; H, 3.28; N, 4.56; S, 5.22

%. Found: C, 53.49; H, 3.45; N, 4.65; S, 5.28 %. **Pd4$_2$** was self-assembled in dmf. Mp. 312 ^{o}C. Selected IR peaks (ATR, cm^{-1}): ν 3071m, 2928m, 1658vs, 1514s, 1247vs, 756vs, 708vs. Anal. calc. for $C_{54}H_{40}Cl_2N_4O_4PdS_2$.3dmf: C, 59.60; H, 4.84; N, 7.72; S, 5.05 %. Found: C, 59.44; H, 4.58; N, 7.37; S, 4.94 %.

***μ*-(Pd5)$_2$:** Ligand **5** (83 mg, 0.22 mmol) and $PdCl_2(CH_3CN)_2$ (60 mg, 0.22 mmol) produced orange-coloured ***μ*-(Pd5)$_2$** with two molecules of co-crystallized $CHCl_3$ according to elemental analyses (120 mg, 92 %). Mp. 323 ^{o}C. Selected IR peaks (KBr, cm^{-1}): ν 3070m, 1595m, 1454s, 851s, 755vs, 704vs. NMR (600 MHz, *d6*-dmso) δ 8.90 (d, *J* = 8.3 Hz, 1H), 8.85 (d, *J* = 8.4 Hz, 2H), 8.64 (dd, *J* = 7.9, 1.1 Hz, 1H), 7.79 – 7.77 (m, 3H), 7.70 – 7.65 (m, 1H), 7.61 (dd, *J* = 5.0, 1.0 Hz, 1H), 7.58 – 7.50 (m, 1H), 7.35 – 7.28 (m, 1H), 7.06 (d, *J* = 7.6 Hz, 1H), 6.99 (dd, *J* = 5.0, 3.8 Hz, 1H), 6.71 (dd, *J* = 3.7, 1.0 Hz, 1H). ESI MS: m/z 1172 [M – Cl]$^{+}$ (35 %, Calc. 1,1172.14), 376 (base peak, ligand). Anal. calc. for $C_{50}H_{32}Cl_4N_4Pd_2S_2$.2$CHCl_3$: C, 46.39; H, 2.55; N, 4.16; S, 4.76 %. Found: C, 46.57; H, 2.75; N, 4.18; S, 4.75 %. **Pd5.acn** was prepared in acetonitrile. Mp. 289 ^{o}C (with decomposition). Selected IR peaks (ATR, cm^{-1}): ν 3078m, 2961m, 1664vs, 1596s, 1514vs, 1247vs, 1023vs, 720vs, 428vs. Anal. calc. for $C_{27}H_{19}Cl_2N_3PdS$: C, 54.52; H, 3.22; N, 7.06; S, 5.39 %. Found: C, 54.85; H, 3.20; N, 7.33; S, 5.32 %. **Pd5.dmf** was also isolated from allowing $PdCl_2(CH_3CN)_2$ and **5** to stand in dmf. Mp. 221 ^{o}C. Selected IR peaks (ATR, cm^{-1}): ν 3072m, 2927m, 1639vs, 1517s, 1360s, 706vs, 428vs. Anal. calc. for $C_{28}H_{23}Cl_2N_3OPdS$: C, 53.65; H, 3.70; N, 6.70; S, 4.77 %. Found: C, 53.55; H, 3.76; N, 7.15; S, 4.77 %.

***μ*-(Pd6)$_2$:** Ligand **6** (60 mg, 0.19mmol) and $PdCl_2(CH_3CN)_2$ (50 mg, 0.19mmol) produced ***μ*-(Pd6)$_2$** (3 mg, 33 %). Mp. 297 ^{o}C. Selected IR peaks (ATR, cm^{-1}): ν 3202s (br), 3070m, 2921w, 1594s, 15.06s, 765s, 602vs. ^{1}H NMR (300 MHz, *d6*-dmso) δ 13.49 (d, *J* = 15.8

Hz, 2H), 7.86 (m, 4H), 7.57 (d, *J* = 6.6 Hz, 2H), 7.44 (m, 4H), 7.35 (s, 12H), 7.00 (d, *J* = 15.0 Hz, 2H), 2.62 (d, *J* = 11.6 Hz, 6H). ESI MS: m/z 987 $[M]^+$ (5 %, Calc. 987.89), 951 (– Cl), 496 (monomer, 100 %), 317 (ligand). Anal. calc. for $C_{40}H_{32}Cl_4N_4Pd_2S_2.2H_2O$: C, 46.94; H, 3.55; N, 5.47; S, 6.26 %. Found: C, 46.85; H, 3.18; N, 5.57; S, 5.73 %.

***μ*-(Pd7)$_2$:** Ligand **7** (200 mg, 0.5 mmol) and $PdCl_2(CH_3CN)_2$ (136 mg, 0.5 mmol) gave ***μ*-(Pd7)$_2$** (201 mg, 67 %). Mp. 343 °C. Selected IR peaks (ATR, cm^{-1}): ν 3203s(br), 3069m, 2921s, 1594s, 1575s, 1455s, 690vs. ^{1}H NMR (400 MHz, *d6*-dmso): δ 13.74 (d, *J* = 22.5 Hz, 1H), 7.93 (d, *J* = 7.3 Hz, 1H), 7.85 (d, *J* = 6.7 Hz, 1H), 7.53 – 7.44 (m, 4H), 7.42 – 7.33 (m, 6H). ESI MS: m/z 1117 $[M]^+$ (5 %, Calc. 1117.67), 520 (monomer – Cl, 100 %), 381 (ligand). Anal. calc. for $C_{38}H_{26}Br_2Cl_4N_4Pd_2S_2$: C, 40.85; H, 2.35; N, 5.01; S, 5.74 %. Found: C, 41.33; H, 2.35; N, 5.08; S, 5.70 %. **Pd7.acn** was obtained by self-assemble of ligand **7** and $PdCl_2(CH_3CN)_2$ in acetonitrile. Mp. 329 °C (with decomposition). Selected IR peaks (ATR, cm^{-1}): ν 3202s (br), 3069m, 2921m, 2851w, 2324w (CH_3CN), 1593s, 1498s, 692vs. ESI MS: m/z 559 $[M – Cl]^+$ (10 %), 521 (– 2Cl, 100 %), 381 (ligand). Anal. calc. for $C_{21}H_{16}BrCl_2N_3PdS.H_2O.{}^1/_4CH_3CN$: C, 41.12; H, 3.01; N, 7.25; S, 5.11 %. Found: C, 41.67; H, 2.94; N, 7.24; S, 4.86 %.

Pd8$_2$: Ligand **8** (72 mg, 0.2 mmol) and $PdCl_2(CH_3CN)_2$ (26 mg, 0.1 mmol) stood in dmf to give crystals of **Pd8$_2$** (65 mg, 72 %). NMR: Solubility in deuterated solvents was bad. ESI MS: m/z 865 $[M – Cl]^+$ (20 %, Calc. 865.09), 830 (100 %, – 2Cl), 363 (ligand). Anal. calc. for $C_{42}H_{36}Cl_2N_4O_4PdS_2.2dmf$: C, 54.99; H, 4.81; N, 8.02; S, 6.12 %. Found: C, 55.13; H, 4.78; N, 8.14; S, 6.00 %.

Pd9.acn: Ligand **9** (100 mg, 0.3 mmol) and $PdCl_2(CH_3CN)_2$ (87 mg, 0.3 mmol) self-assembled to give crystals of **Pd9.acn** (0.14 g, 83 %). Mp. 170 °C ^{1}H NMR (300 MHz, *d6*-dmso): δ 8.09 (dd, *J* = 6.3, 2.7 Hz, 2H), 7.69 – 7.62 (m, 4H), 7.59 – 7.53 (m, 3H), 7.51 – 7.38 (m, 6H), 2.05 (s, 3H, acetonitrile). ESI MS: m/z 481 $[M - Cl]^+$ (18 %, calc. 480.28), 443 (M – 2Cl), 299 (ligand). Anal. calc. for $C_{23}H_{18}Cl_2N_2OPd$: C, 53.57; H, 3.52; N, 5.43 %. Found: C, 53.13; H, 3.54; N, 5.90 %.

Pd10$_2$: Ligand **10** (65 mg, 0.2 mmol), $PdCl_2(CH_3CN)_2$ (45 mg, 0.2 mmol) were reacted as for **μ-(Pd1)$_2$** above, but with only ethanol as solvent to obtain **Pd10$_2$** as orange powder (20 mg, 66 %). Mp. 320 °C. Selected IR peaks (ATR, cm^{-1}): ν 3067m, 2847w, 2768w, 1583s, 1553s, 1454vs, 1129s, 765vs, 696vs. ^{1}H NMR (300 MHz, *d6*-dmso): δ 14.01 (s, 1H), 13.17 (s, 1H), 8.09 (dd, *J* = 15.9, 6.3 Hz, 2H), 8.00 – 7.88 (m, 2H), 7.84 (t, *J* = 7.8 Hz, 2H), 7.64 – 7.55 (m, 2H), 7.49 (m, 6H), 7.38 (d, *J* = 3.4 Hz, 8H), 7.30 (s, 4H). MS (EI) m/z 556 (M^+, 100 %): 556, 778, 660, 587, 515, 351, 297. Anal. calc. for $C_{40}H_{28}Br_2Cl_2N_6Pd.3H_2O$: C, 48.83; H, 3.48; N, 8.54 %. Found: C, 48.88; H, 2.92; N, 8.36 %.

Single crystal X-ray data

The intensity data for the compounds were collected on a Nonius KappaCCD diffractometer using graphite-monochromated Mo-K_α radiation. Data were corrected for Lorentz and polarization effects; absorption was taken into account on a semi-empirical basis using multiple-scans.[41–44] The structures were solved by direct methods (SHELXS) and refined by full-matrix least squares techniques against Fo^2 (SHELXL-97).[44] The hydrogen atoms of the compounds **Pd1.acn** (with exception of the methyle group of C29), **Pd5.acn**, and the hydrogen atoms bonded to the imidazole N of **Pd8.acn**, **Pd8$_2$**, and **Pd10$_2$** were located by difference Fourier synthesis and refined isotropically. All other hydrogen atoms were included at

calculated positions with fixed thermal parameters. All non-hydrogen and non-disordered atoms were refined anisotropically.[44] **Pd8.acn** crystallizes as non-merohedral twins.[45] The twin law is -1 0 0 0 -1 0 0.441 0.139 1. The fractional contribution of the minor component refined to 0.145(2). The program *XP*[46] and *DIAMOND*[47] was used for structure representations.

Catalysis experiments and characterization of biphenyl products

Except for the few higher temperature catalysis experiments, which were carried out under reflux conditions, the ambient condition catalysis runs were routinely conducted in sealed glass vials maintained at 40 – 50 ^{o}C by thermostated oil baths equipped with magnetic stirrers. The substrates boronic acid (1 mmol) and arylbromide reagents (1 mmol) were coupled in the presence of a base additive (1.2 eq.) and palladium catalyst material (0.2 mol %) using water / ethanol mixture (1:3) as reaction media. After the desired duration, an aliquot of the resultant reaction mixture is transferred to a clean vial. The solvent mixture is evaporated under high vacuum suction pressure with cooling trap in place after which the residue is collected in deuterated dmso and transferred into an NMR tube. Yields were routinely estimated by comparison of the NMR signal of the methylene functions on bromophenymethanol and that on the biphenyl coupling product. The catalysis product 1-(4'-(hydroxymethyl)-[1,1'-biphenyl]-4-yl)ethan-1-one has been isolated and characterized.[28] Other new catalysis products were also analysed: 4-(4-methoxyphenyl)pyridine: EI MS: m/z 185 $[M]^+$ (100 %, calc. 185.23), 108 (anisyl), 78 (pyridyl). 4'-methoxy-[1,1'-biphenyl]-2-amine: EI MS: m/z 199 $[M]^+$ (100 %, calc. 199.25), 184 (-methyl). 4,4'-dimethoxy-[1,1'-biphenyl]-2-carboxylic acid: EI MS: m/z 258 $[M]^+$ (100 %, calc. 258.27), 241 (-hzdrodxy), 213 (-carboxy), 152, 106 (anisyl). 4-(benzyloxy)-4'-methoxy-1,1'-biphenyl: EI MS: m/z 290 $[M]^+$ (100 %, calc. 290.36), 199 (-benzyl), 91 (-benzyl). 4,4'-dimethoxy-3-nitro-1,1'-biphenyl: EI MS: m/z 259 $[M]^+$ (100 %, calc. 259.26), 244 (-methyl), 214 (-nitro), 198 (-methyl and nitro), 183 (- 2 methyl and nitro), 168.

(3',5'-dimethyl-[1,1'-biphenyl]-4-yl)methanol: EI MS: m/z 212 $[M]^+$ (100 %, calc. 212.29), 195 (-hydroxy), 183 (- 2methyl).

Estimation of ligand N-donor strength

Typically, protonation equilibrium constant determinations were spectroscopically carried out by UV-Vis or fluorescence measurements using 10^{-5} M solutions of the compounds in ethanol-water mixture (70 % absolute EtOH and 30 % H_2O). A calculated amount of potassium chloride was used to maintain fairly constant ionic strength of 0.1 M. Adjustment of the pH value of the solutions was achieved through the addition of minute volumes of potassium hydroxide or hydrochloric acid solutions and monitored with the aid of Mettler Toledo MPc227 pH/Conductivity Meter calibrated by buffers at pH values of 4.0, 7.0 and 10.1.

Results and discussions

Syntheses of ligands and palladium(II) complexes

The deployment of several ligands (**Scheme 2 (a)**) is with the hope of possibly learning influence of structure-property correlations on the catalytic outcomes. Complexes were also deliberately prepared from various solvent media in order to enable isolating of palladium species in diverse coordination environments. The isolated palladium complexes can be grouped into three variants, which are the mono-ligand complexes that are complemented by coordinated solvent (i.e. **Scheme 2 (b)**, **PdL.acn** and **PdL.dmf**), the mono-ligand complexes that formed Cl-bridged dimers due to absence of coordinating solvent (i.e. **Scheme 2 (c)**, ***μ*-(PdL)$_2$**) and the bis-ligand complexes (i.e. **Scheme 2 (d)**, **PdL$_2$**). Coordinated as well as co-crystallized, non-coordinated solvents were evidenced by X-ray data as well as by their non-stoichiometric amounts in the analytical data of the dried samples. While coordinating solvents

like acetonitrile and dmf generally enabled assembly of the mono-ligand complexes **PdL.acn** and **PdL.dmf** by acting as co-ligands, complexation reactions in poorly coordinating solvents like ethanol generally lead to the chlorido-bridged coordination products ***μ*-(PdL)$_2$**. However, some reactions in dmf also yielded bis-ligand complexes (**Pd4$_2$** and **Pd8$_2$**) [48] while all the methoxy-substituted ligands **3**, **4** and **8** participated in forming the bis-ligand **PdL$_2$** species even when **3** was reacted in acetonitrile under the stoichiometry of 1:1.

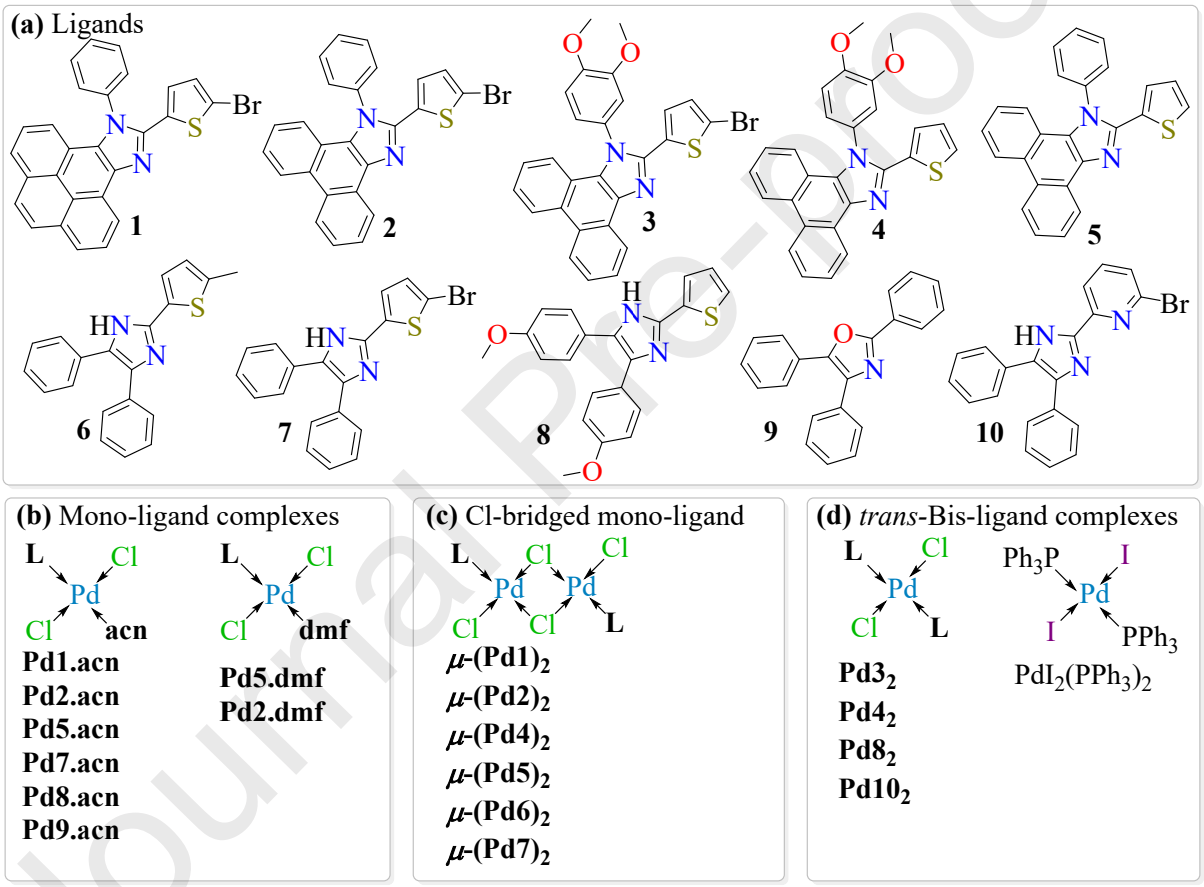

Scheme 2: (a) The investigated ligand frameworks: 2-(thiophen-2-yl)-1H-imidazoles **1** – **8**, 2,4,5-triphenyl-1H-oxazole **9** and 2-(1H-imidazol-2-yl)pyridine **10**. **(b)** Mono-ligand complexes, **(c)** mono-ligand Cl-bridged complexes and **(d)** *trans*-bis-ligand complexes

Single crystal structures

Fig. 1 presents structures for complexes **Pd1.acn**, **Pd5.acn** and **Pd8.acn** while structures of some of the *trans*-bis-ligand complexes **Pd8$_2$**, **Pd10$_2$** and $PdI_2(PPh_3)_2$ are

displayed in **Fig. 2**. Structure refinement details are summarized in **Table 1** while selected bond properties, which are within expected value range,[27,29,49] are collected in **Table 2**. Structures for complexes **Pd2.acn**, **Pd7.acn** and **Pd9.acn** as well as structures of some free ligands were also obtained and presented in the Supplementary Information **Fig. S1** and **Fig. S2**.

It is notable that the Pd–N bond lengths for the bis-ligand $\mathbf{PdL_2}$ species are slightly longer than for the mono-ligand **PdL.acn** analogues, which suggests probable presence of ligand-ligand steric repulsion in the bis-ligand analogues or influence of trans-ligand effects (**Table 2**, **(b)** versus **(a)**). Furthermore, the relative thiophene ring twists away from coplanarity with the imidazole rings, which are larger for the palladium(II) complexes of the phenanthreneyl-substituted ligands (e.g. **Pd1.acn** = 49°, **Pd2.acn** = 47° and **Pd5.acn** = 75°) than for those of the 4,5-diphenyl-substituted ligands (e.g. **Pd7.acn** = 6° or 4°, **Pd8.acn** = 3° or 17° and **Pd9.acn** = 14°), indicate that the phenanthreneyl ligands are the more rigid and sterically demanding ligands. Structure overlays, which were obtained by superimposition of the imidazole ring atoms (C1-N1-C2-C3-N2), illustrate the comparative extents of loss of coplanarity for the complexes relative to the almost complete coplanarity observed in free ligands (**Fig. 3**, see Supplementary Information **Fig. S2**). In summary, rigid and bulky fused-ring ligands are generally favourable for formation of the mono-ligand complexes **PdL.acn** or **PdL.dmf** and their *trans*-bis-ligand coordination products (e.g. $\mathbf{Pd3_2}$ and $\mathbf{Pd4_2}$) can viewed as being more susceptible to dissociation owing to ligand-ligand repulsion.

Continuous Shape Measure calculations (CShM) were carried out on the presented structural geometries to quantitatively analyse the degrees of deviation of the distorted square planer coordination environments from an ideal square planar polyhedron. The results generally indicate minimal deviations with values ranging from 0.279 % to 0.561 % deviations

and the bis ligand complexes displayed slightly lower values relative to the mono-ligand complexes (**Table S2**).

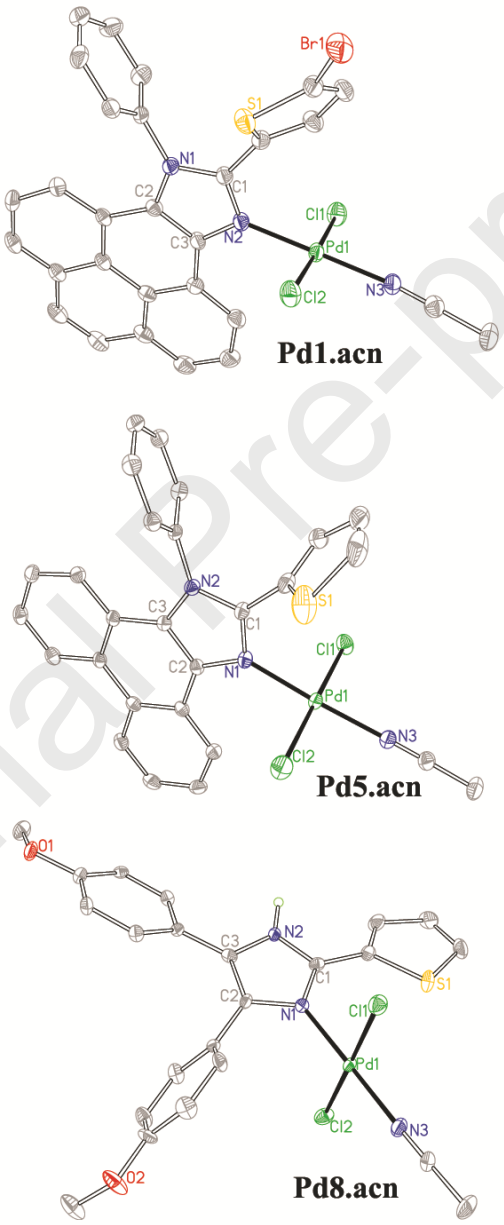

Fig. 1: Structures of complexes **Pd1.acn**, **Pd5.acn** and **Pd8.acn** with thermal ellipsoids drawn at the 50 % probability level. Some protons and non-coordinated solvent molecules have been omitted for clarity.

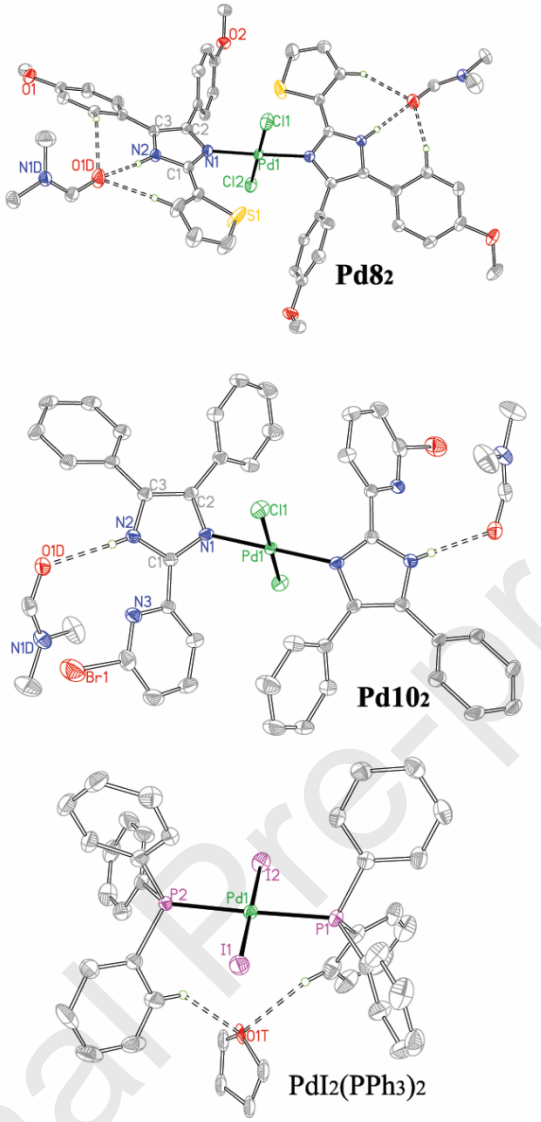

Fig. 2: Structures of complexes **Pd8$_2$**, **Pd10$_2$** and $PdI_2(PPh_3)_2$ with thermal ellipsoids drawn at the 50 % probability level. Some protons and non-coordinated solvent molecules have been omitted for clarity. Hydrogen bonds are shown as dotted bonds.

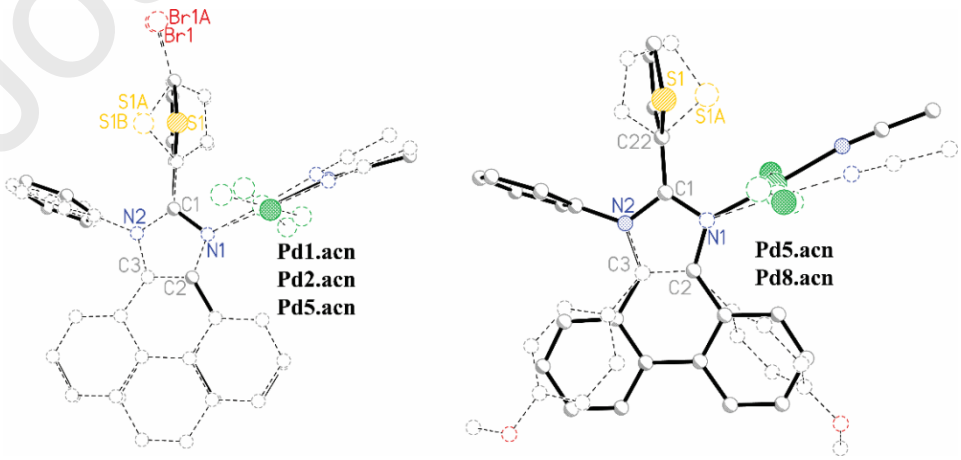

Fig. 3: Structure overlays; the left shows significant thiophene ring twists for **Pd1.acn** and **Pd2.acn** relative to **Pd5.acn**, but the right shows lower twist in **Pd8.acn** compared to **Pd5.acn** (Note: The N-donor labelled N1 in the left overlay represents the N2 atom of **Pd1.acn** and vice versa).

Table 1: Crystal data and refinement details for the X-ray structure determinations.

Parameters	**Pd1.acn**	**Pd5.acn**	**Pd8.acn**	**$Pd8_2$**	**$Pd10_2$**	$PdI_2(PPh_3)_2$
Formula	$C_{31}H_{21}BrCl_2N_4PdS$	$C_{27}H_{19}Cl_2N_3PdS$	$C_{28}H_{28.5}Cl_2N_{5.5}O_2PdS$	$C_{48}H_{50}Cl_2N_6O_6PdS_2$	$C_{46}H_{42}Br_2Cl_2N_8O_2Pd$	$C_{40}H_{38}I_2OP_2Pd$
fw ($g{\cdot}mol^{-1}$)	738.79	594.81	683.42	1048.36	1076.00	956.84
T (°C)	-140(2)	-140(2)	-140(2)	-140(2)	-140(2)	-140(2)
crystal system	monoclinic	orthorhombic	triclinic	monoclinic	monoclinic	monoclinic
space group	P 2_1/n	P b c a	P $\bar{1}$	C 2/c	P 2_1/n	C 2/c
a/ Å	7.6102(1)	9.2523(2)	14.4051(6)	27.3423(7)	13.2553(2)	12.2594(5)
b/ Å	17.5506(4)	16.2106(3)	14.4176(5)	9.8928(3)	9.5124(2)	14.9869(6)
c/ Å	21.8658(3)	32.1392(6)	14.9400(5)	35.5710(9)	17.8364(3)	20.0824(6)
α/°	90.00	90	92.259(2)	90	90	90
β/°	98.4660(10)	90	101.775(2)	95.826(1)	94.493(1)	91.470(2)
γ/°	90.00	90	97.4060(2)	90	90	90
V/Å^3	2888.65(9)	4820.41(16)	3005.30(19)	9572.0(5)	2242.08(7)	3688.5(2)
Z	4	8	4	8	2	4
ρ ($g{\cdot}cm^{-3}$)	1.699	1.639	1.510	1.455	1.594	1.723
μ (cm^{-1})	23.12	11	9	6.42	23.63	22.94
measured data	20928	34536	30760	24412	13429	9643
data with I > 2σ(I)	5783	5145	10382	9803	4597	3454
unique data (R_{int})	6538/0.0419	5467/0.0384	13319/0.0657	10787/0.0269	5132/0.0262	4153/0.0255
wR_2 (all data, on F^2)[a]	0.0713	0.0622	0.1624	0.0759	0.1752	0.1101
R_1 ($I > 2\sigma(I)$)[a]	0.0311	0.0290	0.0710	0.0357	0.0579	0.0400
S [b]	1.087	1.134	1.076	1.093	1.075	1.100
Res. dens./$e{\cdot}Å^{-3}$	0.513/-0.537	0.894/-0.604	2.078/-1.727	0.571/-0.774	2.143/-2.523	1.367/-1.161
absorpt method	multi-scan	multi-scan	multi-scan	multi-scan	multi-scan	multi-scan
absorpt corr $T_{min}/_{max}$	0.5886/0.7456	0.6970/0.7456	0.6452/0.7456	0.6455/0.7456	0.6732/0.7456	0.6009/0.7456

CCDC No.	1821350	1821351	1821352	1821353	1821354	1821355

[a]Definition of the *R* indices: $R_1 = (\Sigma \,||F_o| - |F_c||)/\Sigma|F_o|$; $wR_2 = \{\Sigma[w(F_o^2-F_c^2)^2]/\Sigma[w(F_o^2)^2]\}^{1/2}$ with $w^{-1} = \sigma^2(F_o^2) + (aP)^2+bP$; $P = [2F_c^2 + \text{Max}(F_O^2]/3$; [b)] $s = \{\Sigma[w(F_o^2-F_c^2)^2]/(N_o-N_p)\}^{1/2}$.

Table 2: Bond characteristics around the palladium metal centres of analysed structures

(a) Mono-ligand *trans*-acetonitrile complexes

Complexes	Pd – N	Pd – Cl	Torsion[c]
Pd1.acn	1.999(2), 1.999(2)	2.304(1), 2.299(1)	49.05
Pd2.acn [a]	2.016(2), 1.990(2)	2.305(1), 2.292(1)	47.31
Pd5.acn	2.005(2), 2.004(2)	2.302(1), 2.298(1)	**75.04**
Pd7.acn [a]	1.983(2), 2.008(3)	2.300(1), 2.298(1)	6.39
Pd7.acn [b]	1.999(2), 2.004(3)	2.325(1), 2.283(1)	4.32
Pd8.acn	1.986(5), 2.000(5)	2.308(2), 2.298(2)	3.01
Pd8.acn [b]	1.994(5), 1.996(5)	2.309(2), 2.306(2)	17.52
Pd9.acn [a]	2.001(2), 1.990(2)	2.300(1), 2.290(1)	13.89

(b) Sterically hindered *trans*-bis-ligand complexes

Complexes	Pd – N	Pd – Cl	Torsion[c]
$Pd8_2$	2.025(2), 2.025(2)	2.307(1), 2.307(1)	25.01
$Pd8_2$ [b]	2.044(2), 2.044(2)	2.283(1), 2.306(1)	13.53
$Pd10_2$	2.024(4), 2.024(4)	2.305(1), 2.303(1)	47.19

[a]Structure presented in the Supporting Information **Fig. S1**. [b]Data belong to second crystallographically independent molecule in unit cell. [c]The measure of relative twist of the azole and thiophene rings.

Ligand donor strengths

Knowledge of the ligand N-donor strengths were also pursued in order to obtain probable insight into how they influence electrophilicity of the palladium metal centres, their possible influence on the coordination characteristics and correlation with catalytic trends of the resulting complexes. Using the Henderson-Hasselbalch approximation (**Eqn**. **1**), which becomes simplified to $pH = pK_a$ when $[A^-]$ is equal to [HA], spectroscopic analyses of the protonation-deprotonation equilibrium (**Scheme 3**) enabled estimation of ligand N-donor strengths by focusing on the conjugate acids of the ligands. **Fig. 4** exemplifies the stacked spectra for ligands **3** (left) and **4** (right) with isosbestic features. It is noteworthy that fluorescence measurements are helpful in situations where the UV-Vis spectral profiles are not good enough as for the 4,5-diphenyl-substituted ligands **6** – **8**. The estimated ligand pK_a values are listed in **Table 3** (see Supplementary Information **Fig. S3** for complete spectral stack presentations).

$$pH = pK_a + log_{10}\left(\frac{[A^-]}{[HA]}\right) \quad \textbf{(1)}$$

The estimated pK_a values for the rigid pyreneyl / phenanthreneyl ligands **1**–**5** (pK_a = 1.5 – 2.4) generally suggest weaker N-donor strengths compared to their 4,5-diphenylimidazole analogues **6**–**8** (pK_a = 2.7 – 4.7) (**Table 3**). Since our previous results[36] suggest that substitution at the 1H-imidazole proton does not significantly influence N-donor strengths, the observed difference can be attributed to stronger delocalization of electrons in the phenanthreneyl rings. Within ligands **1**–**5**, the electron-withdrawing influence of the distant bromo-substituent of ligands **1**–**3** appear to be responsible for their lower pK_as (1.5 – 1.9).[38] However, replacement of the imidazole NH group by oxygen as in the oxazole ligand **9** significantly reduces donor strength (i.e. $pK_a \leq 0.8$ for the oxazole **9**).[28,36] Furthermore, it could also be concluded that weaker ligand donor strengths appear to support formation of mono-ligand coordination products then the *trans*-bis-ligand complexation. The significantly weaker donor strengths of the studied ligands relative to the phosphine ligands is also noted.

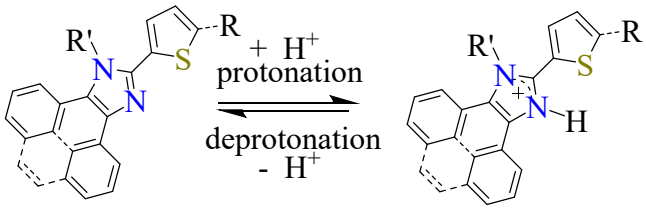

R = H or Br R' = H or Ph derivatives

Scheme 3: A generalized protonation-deprotonation equilibrium at the N-donor of the studied compounds

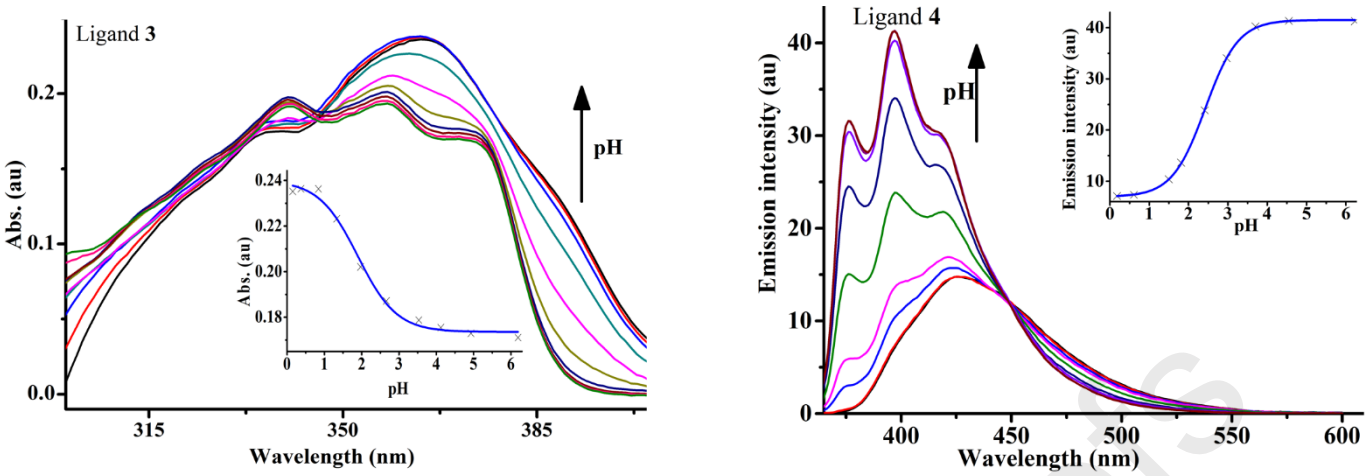

Fig. 4: Representative stacked absorption spectra of ligand **3** and emission spectra of ligand **4** during protonation-deprotonation equilibria. Insets show sigmoid fittings for plots of absorption or emission intensities against pH (**3**, $R^2 = 0.9908$; **4**, $R^2 = 0.9998$).

Table 3: The pK_a estimates of studied ligands

Ligands	pK_a of conjugate acids
1	1.68 ± 0.08
2	1.52 ± 0.05
3	1.90 ± 0.09
4	2.43 ± 0.01[a]
5	2.10 ± 0.02
6	4.65 ± 0.13[a]
7	3.50 ± 0.03[a]
8	2.67 ± 0.10[a]
9	0.84 ± 0.08[a]
$HPPh_3^+$	7.65[b]

[a] These pK_a estimations were done by using fluorescence emission spectra. [b] Data obtained from literature.[50]

Selecting catalytic setting for the complexes

The primary objectives of the catalysis experiments are (i) to study influence of the various coordination environments on coupling catalysis at low temperatures and (ii) to study of influence of ligand differences on the desired catalysis outcomes. Therefore, preliminary catalytic runs were carried out in order to establish a set of reaction conditions to which all the precatalysts would be comparatively subjected. Using 1.0 mmol arylbromide, 1.0 mmol arylboronic acid, 1.2 mmol base additive and 0.2 mol % catalyst material in 4 mL of 3:1 ethanol / water reaction media, the results of catalytic behaviours under varying

conditions were collected using randomly picked members of the palladium precatalyst series and are presented in **Table 4**.

Firstly, after 60 minutes of stirring at temperatures of 20 °C, 30 °C and 40 °C in the presence of the chlorido-bridged, mono-ligand complex ***μ*-(Pd2)$_2$**, it was established that the catalyst becomes active from about 40 °C (entries 1 – 3, **Table 4**). In terms of the temperature regime, such ambient temperature performance is a very significant improvement relative to reported performances by the *trans*-bis-ligand complexes of monodentate N-donors[31–35] as well as performances by the bidentate 2-(1H-imidazol-2-yl)pyridines[27] and 2-(1H-imidazol-2-yl)phenols all of which begin to be active from about 90 °C (**Scheme 1 (c)**).[28,29] Experiments were conducted to further compare temperature-dependence of the catalytic performance within 5 minutes durations for the mono-ligand complexes ***μ*-(Pd1)$_2$**, ***μ*-(Pd2)$_2$** and ***μ*-(Pd4)$_2$** and the results show a similar temperature profile of yield increase versus temperature rise for the three complexes. A steep yield rise around 50 °C is observed for the three complexes (**Fig. 5 (a)**), which suggests that quantitative conversions may be achieved in much lesser than 5 minutes if higher temperatures were deployed. Further reactions conducted at 45 °C also show increasing yields with increasing reaction times is illustrated by **Fig. 5 (b)**, which indicates that the active species are living.

Secondly, positive ligand effect could be established for only the preformed complex ***μ*-(Pd1)$_2$** (48 %) since the *in situ* 'ligand **1** + $PdCl_2(CH_3CN)_2$' approach gave the same 16 % yield as when only the palladium(II) salt $PdCl_2(CH_3CN)_2$ was deployed. With K_2CO_3 as a better base (entries 7 – 11, **Table 4**), it was decided to continue the further reactions at 45 °C and 60 minutes.

Table 4: Results for catalytic performance in the presence of 0.2 mol % of randomly selected pre-catalyst analogues under varying reaction conditions[a]

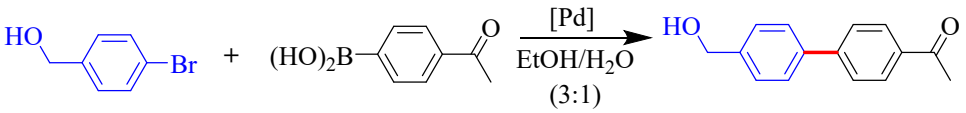

Entry	Catalyst material	Temp. (°C)	Base	Time (min.)	Yield (%)[b]
1	***μ*-(Pd2)$_2$**	20	K_2CO_3	60	3
2	***μ*-(Pd2)$_2$**	30	K_2CO_3	60	4
3	***μ*-(Pd2)$_2$**	45	K_2CO_3	60	43

5	**1** + $PdCl_2(CH_3CN)_2$	40	K_2CO_3	150	16
6	***μ*-(Pd1)$_2$**	40	K_2CO_3	150	48
7	**Pd5.acn**	45	K_2CO_3	60	59
8	**Pd5.acn**	45	None	60	Nill
9	**Pd5.acn**	45	Et_3N	60	4
10	**Pd5.acn**	45	Cs_2CO_3	60	53
11	**Pd5.acn**	45	Na_2CO_3	60	54

[a]Common reaction conditions: 1.0 mmol of (4-acetylphenyl)boronic acid; 1.0 mmol of (4-bromophenyl)methanol; 0.2 mol % catalyst loading; 1.2 mmol base additive; Solvent media is 4 mL of 3:1 ethanol/H_2O mixture. [b]Yields are estimated by ^{1}H-NMR and reported to the nearest whole number.

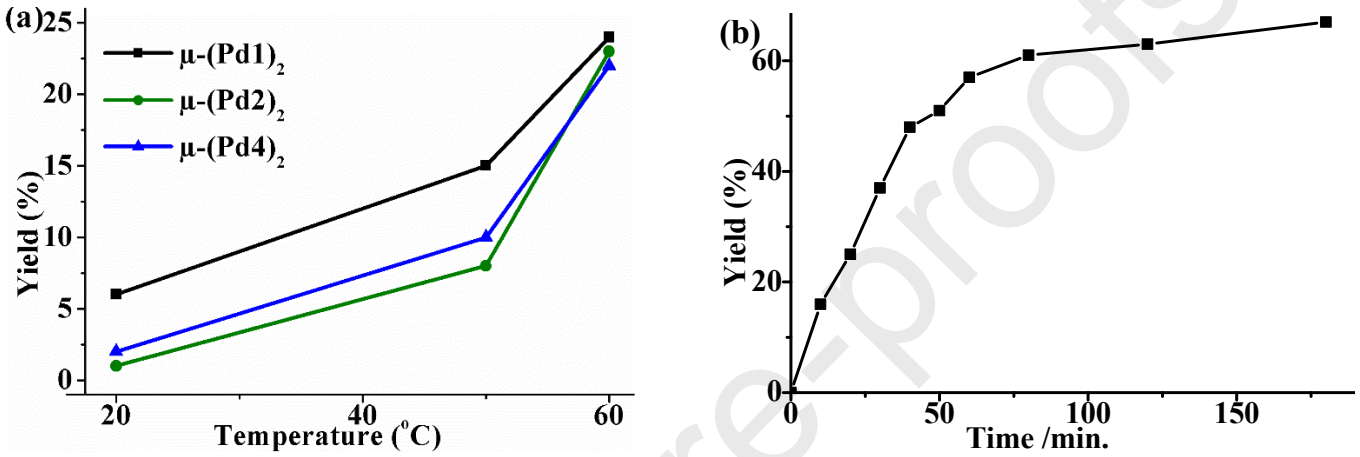

Fig. 5: (a) Catalyst activity change as a function of reaction temperature for ***μ*-(Pd1)$_2$**, ***μ*-(Pd2)$_2$** and ***μ*-(Pd4)$_2$** under 5 minutes; (b) Plot of reaction yield for ***μ*-(Pd5)$_2$** against reaction time at 45 °C. Reaction conditions: 1 mmol of both coupling partner substrates, 0.2 mol % catalyst, 1.2 eq. K_2CO_3.

Comparison of catalysis by coordination environments and ligand properties

In order to comparatively analyse influence of the different coordination modes and ligand variations on catalytic outcomes under ambient temperatures, 1.0 mmol of both (4-acetylphenyl)boronic acid and (4-bromophenyl)methanol, 0.2 mol % catalyst loading and 1.2 mmol K_2CO_3 in 3:1 ethanol/H_2O mixture (4 mL) were stirred at 45 °C for 60 minutes. The catalysis results are shown in **Fig. 6** as a bar chart of turnover frequencies (TOFs) and the corresponding table of data is provided in Supplementary Information **Table S1**. In our focus on monodentate N-donor ligands, three key conclusions could be drawn.

Firstly, the *trans*-bis-ligand pre-catalysts (i.e. **PdL$_2$**) generally performed poorer than the mono-ligand analogues (i.e. **PdL.acn**, **PdL.dmf** or ***μ*-(PdL)$_2$**). While $PdI_2(PPh_3)_2$, which is similar to the popular phosphine-based coupling catalyst, offered no observable catalyst activity at 45 °C temperature regime, the

bis-ligand complexes **Pd8$_2$** and **Pd10$_2$** gave only 13 % and 6 % yields, respectively (**Fig. 6**, **Table S1**). The higher TOF values obtained for the bis-ligand complexes **Pd3$_2$** and **Pd4$_2$** could be attributed to their ease of decomposing into mono-ligand species, which is consequent on ligand-ligand repulsions between the bulky and weakly donating phenanthreneyl ligands. That the **PdL$_2$** systems could generate active species at all while $PdI_2(PPh_3)_2$ generates none is arguably attributable to the much stronger donor strength of the triphenylphosphine ligand. Therefore, it could be concluded that (i) the *trans*-bis-ligand coordination remarkably hinders ambient temperature generation of active palladium centres and that (ii) the stronger the donor strength of monodentate ligands in *trans*-bis-ligand complexation, the worse the chances of functioning as a catalyst for the ambient temperature regimes becomes.

Secondly, comparing among the catalytically productive mono-ligand complexes **PdL.acn**, **PdL.dmf** and ***μ*-(PdL)$_2$** in **Fig. 6**, complexes of the flexible 4,5-diphenyl-substituted ligands displayed relatively weaker efficiencies (i.e. **Pd7.acn**, **Pd8.acn** and **Pd9.acn** compared to **Pd1.acn** – **Pd5.acn**; ***μ*-(Pd6)$_2$** and ***μ*-(Pd7)$_2$** compared to ***μ*-(Pd1)$_2$** - ***μ*-(Pd5)$_2$**). Therefore, rigidity or bulkiness of the ligand frameworks appears to be important for the low temperature catalysis. The highest TON value observed from the complexes of ligand **5** (i.e. **Pd5.acn** and ***μ*-(Pd5)$_2$**) may probably be associated with the larger extent of out of plane thiophene ring twist.

Thirdly, acetonitrile as complementary ligand appears more favourable for active catalyst generation than dmf or the chlorido-bridging coordination. In summary, the ambient temperature performance can be considered successful for the mono-ligand dihalopalladium(II) complex designs supported by monodentate N-donor ligand and complemented by an easily detachable solvent co-ligand. On the other hand, the use of more than 1:1 ligand equivalents in palladium catalysis, which can be viewed as imparting negative influence on the catalytic behaviour of palladium centre, should be avoided if ambient temperature catalyst reactivities is desired.[51] As outlook, the design of strongly coordinating N-donors with steric features capable of hindering bis-ligand complexation may be the way to go for designing N-supported palladium precatalysts. **Scheme 4** presents results that generally indicate substituent tolerance.

However, while single *ortho*-substituted aryl bromide was easily coupled, the 2,6-disubstituted aryl bromide yielded negligible coupling products. Trace of activated aryl chloride coupling was also observed at 60 °C by complex **Pd1.acn** (see also **Fig. S4** of the Supplementary Information).

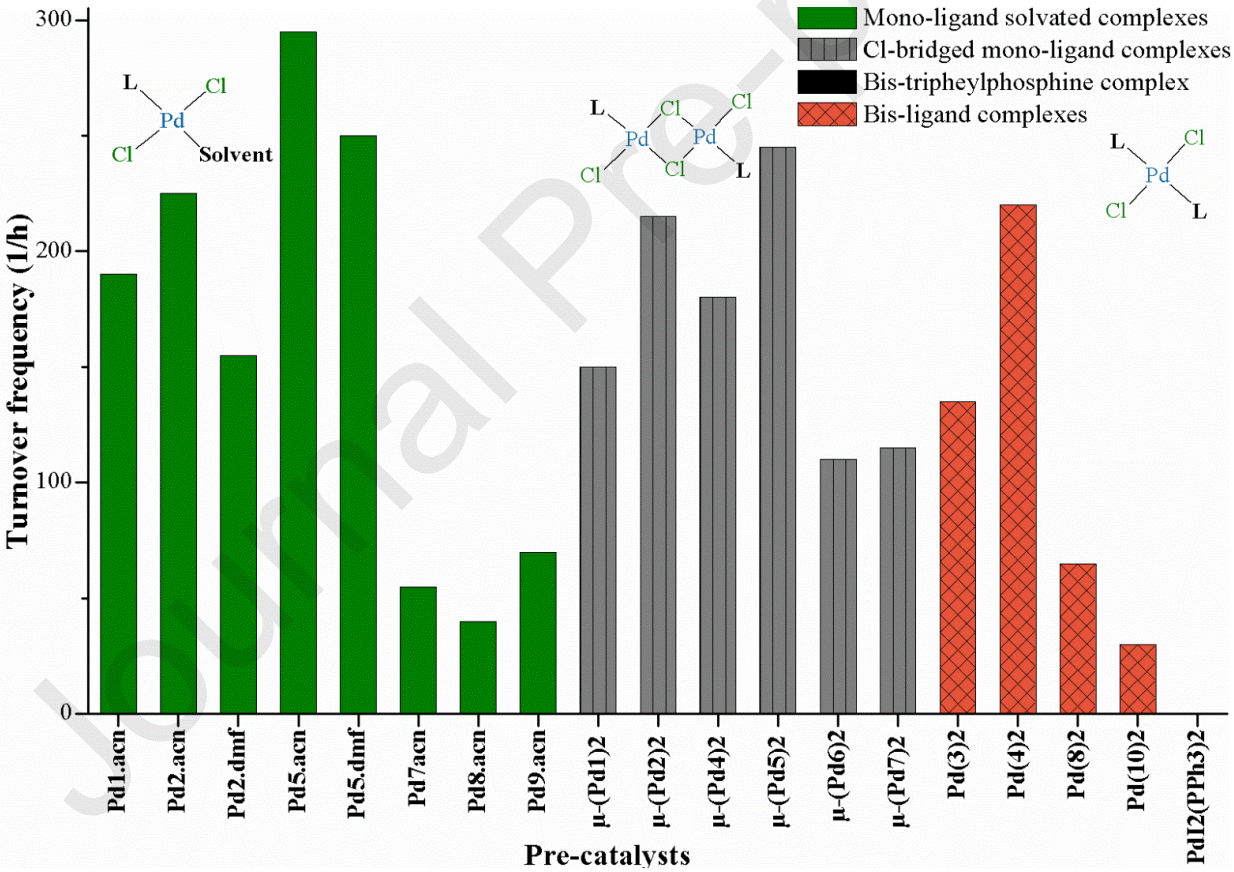

Fig. 6: Catalytic performance for the series of precatalyst probe complexes. [a]Reaction conditions: 1 mmol of (4-acetylphenyl)boronic acid; 1 mmol of (4-bromophenyl)methanol; 1.2 equivalent of K_2CO_3; 0.2 mol % of palladium complex loading; Solvent media, 4 mL of 3:1 solvent/H_2O mixture.; 45 °C; 1hr. [b]Yield determined by ^{1}H-NMR spectroscopy

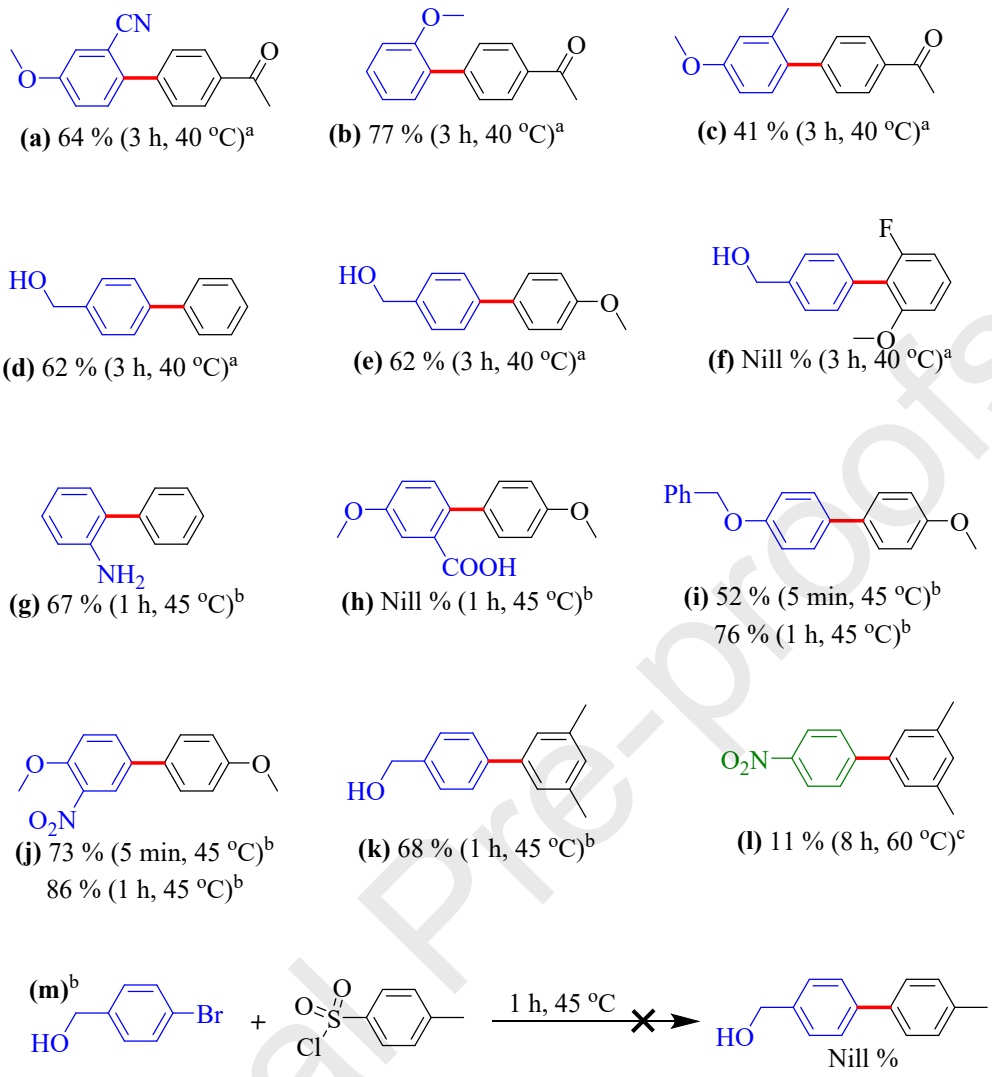

Scheme 4: Coupling reactions with various substrates (Reaction conditions: 1 mmol of boronic acid reagent; 1 mmol of aryl bromide reagent; 1.2 equivalent of K_2CO_3; 0.2 mol % of palladium complex loading; Solvent media, 4 mL of 3:1 EtOH/H_2O mixture; Yield determined by ^{1}H-NMR. [a]Catalyzed by ***μ*-(Pd1)$_2$**; [b]Catalyzed by 0.2 mol % of **Pd1.acn**; [c]Catalyzed by 1 mol % of **Pd1.acn**.)

Conclusions

Monodentate 2-(thiophen-2-yl)-1H-imidazoles **1** – **8**, 2,4,5-triphenyloxazole **9** and 2-(1H-imidazol-2-yl)pyridine **10** have been prepared to study N-donor ligand frameworks towards ambient temperature functionality of palladium species in coupling catalysis. Their corresponding palladium complexes were obtained in three coordination environments: (i) the mono-ligand **PdL.acn** or **PdL.dmf**

complexes complemented by *trans*-solvent coordination, (ii) the chlorido-bridged dimers $\boldsymbol{\mu}$**-(PdL)$_2$** and (iii) the *trans*-bis-ligand complexes **PdL$_2$**. Ligand donor strengths were estimated as pK_as.

In general, while the rigid and weaker donor ligands easily formed stable mono-ligand mono-solvent complexes **PdL.acn** or **PdL.dmf**, the more flexible and stronger donor ligands showed some extent of preference for *trans*-bis-ligand **PdL$_2$** complexation. The mono-ligand pre-catalysts are able to efficiently generate living active palladium catalysts from about 40 ^oC. This performance is a very significant ambient temperature catalyst improvement relative to performances reported for analogous complexes bearing monodentate N-donors in *trans*-bis-ligand N-donors or complexes of multidentate ligands. Results show functional group tolerance and even coupling of activated aryl chloride could also be observed at 60 ^oC. The respected phosphine ligand (PPh_3) in *trans*-bis-ligand complexation displayed no yield under the same low temperature conditions where the designed complexes were efficient.

From the observed catalysis trends, it was concluded that strong donors in *trans*-bis-ligand coordination environments remarkably hinder catalyst generation possibilities at ambient temperatures and is responsible for having to use very high temperatures, many hours of reflux and excessive catalyst loadings. Therefore, it was concluded that every route to formation of *trans*-bis-ligand complexation, which is often ignorantly triggered when two or more ligand equivalents to palladium are applied, should be avoided. An outlook of stronger monodentate N-donor ligand designs with sufficient steric bulkiness, which would hinder bis-ligand complexation, is being considered.

Supplementary Information

Further structural and spectroscopic data are available in the supplementary information. Crystallographic data (excluding structure factors) has been deposited with the Cambridge Crystallographic Data Centre as supplementary publication bearing CCDC-1821350 for **Pd1.acn**, CCDC-1821351 for **Pd5.acn**, CCDC-

1821352 for **Pd8.acn**, CCDC-1821353 for **$Pd8_2$**, CCDC-1821354 for **$Pd10_2$**, and CCDC-1821355 for $PdI_2(PPh_3)_2$.

Conflict of interest

All authors are aware of the submission and agree to its publication without conflicts of intersts.

Acknowledgements

A.O.E is grateful to the Alexander von Humboldt Foundation for support through Georg-Forster postdoctoral scholarship and to Redeemer's University for allowing fellowship leave. The financial support by the Deutsche Forschungsgemeinschaft (DFG) is gratefully acknowledged (PL 155/11, PL 155/12 and PL155/13).

REFENECES

References

[1] H. Zhang, P. Ruiz-Castillo, S.L. Buchwald, Palladium-Catalyzed C-O Cross-Coupling of Primary Alcohols, Org. Lett. 20 (2018) 1580–1583. https://doi.org/10.1021/acs.orglett.8b00325.

[2] I. Sarhid, I. Abdellah, C. Martini, V. Huc, D. Dragoe, P. Beaunier, I. Lampre, H. Remita, Plasmonic catalysis for the Suzuki–Miyaura cross-coupling reaction using palladium nanoflowers, New J. Chem. 43 (2019) 4349–4355. https://doi.org/10.1039/C8NJ06370B.

[3] E.O. Pentsak, V.P. Ananikov, Pseudo-Solid-State Suzuki-Miyaura Reaction and the Role of Water Formed by Dehydration of Arylboronic Acids, Eur. J. Org. Chem. 2019 (2019) 4239–4247. https://doi.org/10.1002/ejoc.201900410.

[4] V. Sharma, S. Kumar, A. Bahuguna, D. Gambhir, P.S. Sagara, V. Krishnan, Plant leaves as natural green scaffolds for palladium catalyzed Suzuki-Miyaura coupling reactions, Bioinspir. Biomim. 12 (2016) 16010–16017. https://doi.org/10.1088/1748-3190/12/1/016010.

[5] V.B. Saptal, M.V. Saptal, R.S. Mane, T. Sasaki, B.M. Bhanage, Amine-Functionalized Graphene Oxide-Stabilized Pd Nanoparticles (Pd@APGO): A Novel and Efficient Catalyst for the Suzuki and Carbonylative Suzuki-Miyaura Coupling Reactions, ACS Omega 4 (2019) 643–649. https://doi.org/10.1021/acsomega.8b03023.

[6] B. Guo, H.-X. Li, C.-H. Zha, D.J. Young, H.-Y. Li, J.-P. Lang, Visible-Light-Enhanced Suzuki-Miyaura Reactions of Aryl Chlorides in Water with Pd NPs Supported on a Conjugated Nanoporous Polycarbazole, ChemSusChem 12 (2019) 1421–1427. https://doi.org/10.1002/cssc.201802918.

[7] M. Duss, J.J. Vallooran, L. Salvati Manni, N. Kieliger, S. Handschin, R. Mezzenga, H.J. Jessen, E.M. Landau, Lipidic Mesophase-Embedded Palladium Nanoparticles: Synthesis and Tunable Catalysts in Suzuki-Miyaura Cross-Coupling Reactions, Langmuir 35 (2019) 120–127. https://doi.org/10.1021/acs.langmuir.8b02905.

[8] Y. Zhao, L. Du, H. Li, W. Xie, J. Chen, Is the Suzuki-Miyaura Cross-Coupling Reaction in the Presence of Pd Nanoparticles Heterogeneously or Homogeneously Catalyzed? An Interfacial Surface-Enhanced Raman Spectroscopy Study, J. Phys. Chem. Lett. 10 (2019) 1286–1291. https://doi.org/10.1021/acs.jpclett.9b00351.

[9] P. Destito, A. Sousa-Castillo, J.R. Couceiro, F. López, M.A. Correa-Duarte, J.L. Mascareñas, Hollow nanoreactors for Pd-catalyzed Suzuki-Miyaura coupling and O-propargyl cleavage reactions in bio-relevant aqueous media, Chem. Sci. 10 (2019) 2598–2603. https://doi.org/10.1039/C8SC04390F.

[10] H. Ma, C. Bai, Y.-S. Bao, Heterogeneous Suzuki–Miyaura coupling of heteroaryl ester via chemoselective C(acyl)–O bond activation, RSC Adv. 9 (2019) 17266–17272. https://doi.org/10.1039/C9RA02394A.

[11] L.L. Liu, P. Chen, Y. Sun, Y. Wu, S. Chen, J. Zhu, Y. Zhao, Mechanism of Nickel-Catalyzed Selective C-N Bond Activation in Suzuki-Miyaura Cross-Coupling of Amides: A Theoretical Investigation, J. Org. Chem. 81 (2016) 11686–11696. https://doi.org/10.1021/acs.joc.6b02093.

[12] J.W. Lehmann, I.T. Crouch, D.J. Blair, M. Trobe, P. Wang, J. Li, M.D. Burke, Axial shielding of Pd(II) complexes enables perfect stereoretention in Suzuki-Miyaura cross-coupling of Csp3 boronic acids, Nat. commun. 10 (2019) 1263. https://doi.org/10.1038/s41467-019-09249-z.

[13] N. Ye, W.-M. Dai, An Efficient and Reliable Catalyst System Using Hemilabile Aphos for B -Alkyl Suzuki-Miyaura Cross-Coupling Reaction with Alkenyl Halides, Eur. J. Org. Chem. 2013 (2013) 831–835. https://doi.org/10.1002/ejoc.201201602.

[14] B. Atwater, N. Chandrasoma, D. Mitchell, M.J. Rodriguez, M.G. Organ, Pd-PEPPSI-IHept(Cl) A General-Purpose, Highly Reactive Catalyst for the Selective Coupling of Secondary Alkyl Organozincs, Chem. Eur. J. 22 (2016) 14531–14534. https://doi.org/10.1002/chem.201603603.

[15] M. Pompeo, R.D.J. Froese, N. Hadei, M.G. Organ, Pd-PEPPSI-IPent(Cl): a highly effective catalyst for the selective cross-coupling of secondary organozinc reagents, Angew. Chem. Intl. Edit. 51 (2012) 11354–11357. https://doi.org/10.1002/anie.201205747.

[16] Z. Lu, J.B. Jasinski, S. Handa, G.B. Hammond, Recyclable cellulose-palladium nanoparticles for clean cross-coupling chemistry, Org. Biomol. Chem. 16 (2018) 2748–2752. https://doi.org/10.1039/C8OB00527C.

[17] J.D. Hicks, A.M. Hyde, A.M. Cuezva, S.L. Buchwald, Pd-catalyzed N-arylation of secondary acyclic amides: catalyst development, scope, and computational study, J. Am. Chem. Soc. 131 (2009) 16720–16734. https://doi.org/10.1021/ja9044357.

[18] J. Xu, R.Y. Liu, C.S. Yeung, S.L. Buchwald, Monophosphine Ligands Promote Pd-Catalyzed C–S Cross-Coupling Reactions at Room Temperature with Soluble Bases, ACS Catal. 9 (2019) 6461–6466. https://doi.org/10.1021/acscatal.9b01913.

[19] P.R. Melvin, D. Balcells, N. Hazari, A. Nova, Understanding Precatalyst Activation in Cross-Coupling Reactions: Alcohol Facilitated Reduction from Pd(II) to Pd(0) in Precatalysts of the

Type (η 3 -allyl)Pd(L)(Cl) and (η 3 -indenyl)Pd(L)(Cl), ACS Catal. 5 (2015) 5596–5606. https://doi.org/10.1021/acscatal.5b01291.

[20] M.A. Topchiy, A.F. Asachenko, M.S. Nechaev, Solvent-Free Buchwald-Hartwig Reaction of Aryl and Heteroaryl Halides with Secondary Amines, Eur. J. Org. Chem. 2014 (2014) 3319–3322. https://doi.org/10.1002/ejoc.201402077.

[21] Y. Yang, J.F.Y. Lim, X. Chew, E.G. Robins, C.W. Johannes, Y.H. Lim, H. Jong, Palladium precatalysts containing meta-terarylphosphine ligands for expedient copper-free Sonogashira cross-coupling reactions, Catal. Sci. Technol. 5 (2015) 3501–3506. https://doi.org/10.1039/C5CY00507H.

[22] J.-M. Collinson, J.D.E.T. Wilton-Ely, S. Díez-González, Functionalised [(NHC)Pd(allyl)Cl] complexes: Synthesis, immobilisation and application in cross-coupling and dehalogenation reactions, Catal. Commun. 87 (2016) 78–81. https://doi.org/10.1016/j.catcom.2016.09.006.

[23] D. Bulfield, S.M. Huber, Synthesis of Polyflourinated Biphenyls; Pushing the Boundaries of Suzuki–Miyaura Cross Coupling with Electron-Poor Substrates, J. Org. Chem. 82 (2017) 13188–13203. https://doi.org/10.1021/acs.joc.7b02267.

[24] N.C. Bruno, M.T. Tudge, S.L. Buchwald, Design and preparation of new palladium precatalysts for C–C and C–N cross-coupling reactions, Chem. Sci. 4 (2013) 916–920. https://doi.org/10.1039/C2SC20903A.

[25] M. Yamaguchi, K. Manabe, Three-step synthesis of 2,5,7-trisubstituted indoles from N-acetyl-2,4,6-trichloroaniline using Pd-catalyzed site-selective cross-coupling, Org. Biomol. Chem. 15 (2017) 6645–6655. https://doi.org/10.1039/c7ob01547j.

[26] T. Si, B. Li, W. Xiong, B. Xu, W. Tang, Efficient cross-coupling of aryl/alkenyl triflates with acyclic secondary alkylboronic acids, Org. Biomol. Chem. 15 (2017) 9903–9909. https://doi.org/10.1039/c7ob02531a.

[27] A.O. Eseola, D. Geibig, H. Görls, W.-H. Sun, X. Hao, J.A.O. Woods, W. Plass, Palladium(II) complexes bearing 2-(1H-imidazol/oxazol-2-yl)-pyridines: Synthesis, structures and ligand effects in Suzuki–Miyaura cross-coupling, J. Organomet. Chem. 754 (2014) 39–50. https://doi.org/10.1016/j.jorganchem.2013.12.041.

[28] A.O. Eseola, O. Akogun, H. Görls, O. Atolani, G.A. Kolawole, W. Plass, Ligand characteristics and in situ generation of Pd active species towards CC coupling using series of 2-(1H-imidazol-2-yl)phenols, J. Mol. Catal. A. Chem. 387 (2014) 112–122. https://doi.org/10.1016/j.molcata.2014.02.032.

[29] A.O. Eseola, H. Görls, J.A.O. Woods, W. Plass, Cyclometallation, steric and electronic tendencies in a series of Pd(II) complex pre-catalysts bearing imidazole–phenol ligands and effects on Suzuki–Miyaura catalytic efficiencies, J. Mol. Catal. A. Chem. 406 (2015) 224–237. https://doi.org/10.1016/j.molcata.2015.06.001.

[30] A.O. Eseola, H. Görls, W. Plass, Importance of monodentate mono-ligand designs in developing N-stabilized Pd catalysts for efficient ambient temperature C C coupling: Donor strengths and steric features, Mol. Catal 473 (2019) 110398. https://doi.org/10.1016/j.mcat.2019.110398.

[31] J. Wiedermann, K. Mereiter, K. Kirchner, Palladium imine and amine complexes derived from 2-thiophenecarboxaldehyde as catalysts for the Suzuki cross-coupling of aryl bromides, J. Mol. Catal. A-Chem. 257 (2006) 67–72. https://doi.org/10.1016/j.molcata.2006.04.009.

[32] E. Ocansey, J. Darkwa, B.C.E. Makhubela, Synthesis, characterization and evaluation of bulky bis(pyrazolyl)palladium complexes in Suzuki–Miyaura cross-coupling reactions, RSC Adv. 8 (2018) 13826–13834. https://doi.org/10.1039/C8RA01430B.

[33] K. Kawamura, S. Haneda, Z. Gan, K. Eda, M. Hayashi, 2-Phenylimidazole−PdCl 2 and 2-Phenylimidazoline−PdCl 2 Complexes: Single-Crystal and Powder X-ray Diffractometry, 1 H NMR Spectra, and Comparison of Catalytic Activities in Coupling Reactions †, Organometallics 27 (2008) 3748–3752. https://doi.org/10.1021/om800230y.

[34] C. Xi, Y. Wu, X. Yan, cis-Fashioned palladium (II) complexes of 2-phenylbenzimidazole ligands: Synthesis, characterization, and catalytic behavior towards Suzuki–Miyaura reaction, J. Organomet. Chem. 693 (2008) 3842–3846. https://doi.org/10.1016/j.jorganchem.2008.09.042.

[35] J.-C. Xiao, B. Twamley, J.'n.M. Shreeve, An ionic liquid-coordinated palladium complex: a highly efficient and recyclable catalyst for the Heck reaction, Org. Lett. 6 (2004) 3845–3847. https://doi.org/10.1021/ol048327i.

[36] A.O. Eseola, W. Li, O.G. Adeyemi, N.O. Obi-Egbedi, J.A.O. Woods, Hemilability of 2-(1H-imidazol-2-yl)pyridine and 2-(oxazol-2-yl)pyridine ligands: Imidazole and oxazole ring Lewis basicity, Ni(II)/Pd(II) complex structures and spectra, Polyhedron 29 (2010) 1891–1901. https://doi.org/10.1016/j.poly.2010.02.039.

[37] A.O. Eseola, N.O. Obi-Egbedi, Spectroscopic study of 2-, 4- and 5-substituents on pKa values of imidazole heterocycles prone to intramolecular proton-electrons transfer, Spectrochim. Acta A. 75 (2010) 693–701. https://doi.org/10.1016/j.saa.2009.11.041.

[38] A.O. Eseola, O. Adepitan, H. Görls, W. Plass, Electronic/substituents influence on imidazole ring donor–acceptor capacities using 1H-imidazo[4,5-f][1,10]phenanthroline frameworks, New J. Chem. 36 (2012) 891–902. https://doi.org/10.1039/C2NJ20880F.

[39] S. Demir, B. Eren, M. Hołyńska, (1-Methyl-2-(thiophen-2-yl)-1H-benzo[d]imidazole) and its three copper complexes: Synthesis, characterization and fluorescence properties, J. Mol. Str. 1081 (2015) 304–310. https://doi.org/10.1016/j.molstruc.2014.10.043.

[40] E.R.R. Young, R.L. Funk, A Practical Synthesis of Pyrene-4,5-dione, J. Org. Chem. 63 (1998) 9995–9996. https://doi.org/10.1021/jo970344g.

[41] Nonius B.V., COLLECT: Data Collection Software, Netherlands, 1998.

[42] Z. Otwinowski, Minor, W. in Carter, C. W., R.M. Sweet (Eds.), Macromolecular Crystallography Part A: Processing of X-Ray Diffraction Data Collected in Oscillation Mode, Academic Press, 1997.

[43] Bruker-AXS inc., SADABS, Madison, WI, U.S.A., 2002.

[44] G.M. Sheldrick, A short history of SHELX, Acta Crystallogr. A. 64 (2008) 112–122. https://doi.org/10.1107/S0108767307043930.

[45] A.L. Spek, PLATON SQUEEZE: A tool for the calculation of the disordered solvent contribution to the calculated structure factors, Acta Crystallogr. C. 71 (2015) 9–18. https://doi.org/10.1107/S2053229614024929.

[46] Siemens Analytical X-ray Instruments Inc., Siemens (1994). XP: Interactive Molecular Graphics Program, Madison, Winscosin, USA, 1994.

[47] Dr. H. Putz & Dr. K. Brandenburg GbR, Kreuzherrenstr. 102, 53227 Bonn, Germany, Diamond: Crystal and Molecular Structure Visualization, Crystal Impact.

[48] M. Munakata, S. Kitagawa, M. Miyazima, Classification of solvents based on their coordination power to nickel(II) ion. A new measure for solvent donor ability, Inorg. Chem. 24 (1985) 1638–1643. https://doi.org/10.1021/ic00205a009.

[49] A. Zatajska, M. Siczek, A. Skarżyńska, P. Smoleński, New water-soluble palladium(II) iodide complexes derived from N-protonated or N-alkyl-1,3,5-triaza-7-phosphaadamantanes:

Synthesis, crystal structure and catalytic properties in aqua media, Inorg. Chim. Acta. 455 (2017) 701–706. https://doi.org/10.1016/j.ica.2016.03.041.

[50] K. Haav, J. Saame, A. Kütt, I. Leito, Basicity of Phosphanes and Diphosphanes in Acetonitrile, Eur. J. Org. Chem. 2012 (2012) 2167–2172. https://doi.org/10.1002/ejoc.201200009.

[51] H. Wang, X. Zhang, P. Tang, Total syntheses of schilancidilactones A and B, schilancitrilactone A, and 20-epi-schilancitrilactone A via late-stage nickel-catalyzed cross coupling, Chem. Sc. 8 (2017) 7246–7250. https://doi.org/10.1039/c7sc03293e.

Dr. Abiodun Omokehinde Eseola: Conceptualization; Data curation; Formal analysis; Funding acquisition (Alexander von Humboldt Postdoctoral Scholarship); Investigation; Methodology; Project administration; Resources; Software; Supervision; Validation; Visualization; Roles/Writing - original draft; Writing - review & editing

Dr. Helmar Görls: Data curation; Resources

Prof. Joseph A. O Woods: Supervision; Visualization; Writing - review & editing

Prof. Winfried Plass: Funding acquisition; Project administration; Resources; Supervision; Visualization

Declaration of interests

☒ The authors declare that they have no known competing financial interests or personal relationships that could have appeared to influence the work reported in this paper.

☐The authors declare the following financial interests/personal relationships which may be considered as potential competing interests:

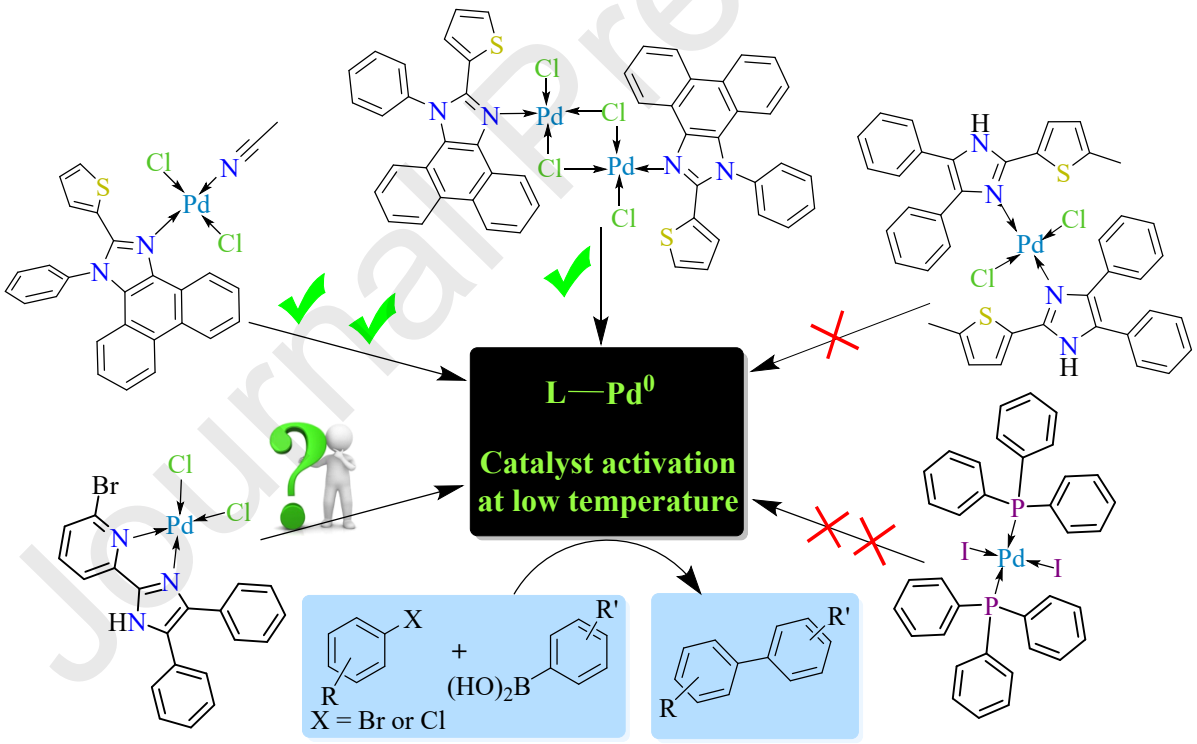

Synopsis

The coordinative saturation around the palladium centre is determinant for possibility of participation in low temperature catalysis.

Highlights

- Series of monodentate 2-(thiophen-2-yl)-1H-imidazole ligand, which have varying donor strengths and steric features, were studied.
- Relative to known N-stabilized palladium catalysts, the reported activities at as low as 40 ^{o}C represents improvement.
- It was established that trans-bis-ligand coordination utterly hinders usefulness of precatalysts at ambient temperatures.
- Use of multiple ligand equivalents in precatalysts or as *in situ* 'ligand + palladium salt' species should be discouraged.